

Distribution of microglia/immune cells in the brain of adult zebrafish in homeostatic and regenerative conditions: Focus on oxidative stress during brain repair

Sai Sandhya Narra¹ | Philippe Rondeau¹ | Danielle Fernezelian¹ | Laura Gence¹ |
Batoul Ghaddar¹ | Emmanuel Bourdon¹ | Christian Lefebvre d'Hellencourt¹ |
Sepand Rastegar²  | Nicolas Diotel¹ 

¹Université de La Réunion, INSERM, UMR 1188, Diabète athérombose Thérapies Réunion Océan Indien (DéTROI), Saint Denis de La Réunion, France

²Institute of Biological and Chemical Systems Biological Information Processing (IBCS BIP), Karlsruhe Institute of Technology (KIT), Karlsruhe, Germany

Correspondence

Nicolas Diotel, Université de La Réunion, INSERM, UMR 1188, Diabète athérombose Thérapies Réunion Océan Indien (DéTROI), Saint Denis de La Réunion, France.
Email: nicolas.diotel@univ-reunion.fr

Funding information

University of La Réunion European Union (EU) Région Réunion French State, Grant/Award Number: FEDER RE0022527 (ZEBRATOX)

Abstract

Microglia are macrophage-like cells exerting determinant roles in neuroinflammatory and oxidative stress processes during brain regeneration. We used zebrafish as a model of brain plasticity and repair. First, by performing L-plastin (Lcp1) immunohistochemistry and using transgenic Tg(*mpeg1.1:GFP*) or Tg(*mpeg1.1:mCherry*) fish, we analyzed the distribution of microglia/immune cells in the whole brain. Specific regional differences were evidenced in terms of microglia/immune cell density and morphology (elongated, branched, highly branched, and amoeboid). Taking advantage of Tg(*fli:GFP*) and Tg(*GFAP::GFP*) enabling the detection of endothelial cells and neural stem cells (NSCs), we highlighted the association of elongated microglia/immune cells with blood vessels and rounded/amoeboid microglia with NSCs. Second, after telencephalic injury, we showed that L-plastin cells were still abundantly present at 5 days post-lesion (dpl) and were associated with regenerative neurogenesis. Finally, RNA-sequencing analysis from injured telencephalon (5 dpl) confirmed the upregulation of microglia/immune cell markers and highlighted a significant increase of genes involved in oxidative stress (*nox2*, *nrf2a*, and *gsr*). The analysis of antioxidant activities at 5 dpl also revealed an upregulation of superoxide dismutase and persistent H₂O₂ generation in the injured telencephalon. Also, microglia/immune cells were shown to be a source of oxidative stress at 5 dpl. Overall, our data provide a better characterization of microglia/immune cell distribution in the healthy zebrafish brain, highlighting some evolutionarily conserved features with mammals. They also emphasize that 5 days after injury, microglia/immune cells are still activated and are associated to a persistent redox imbalance. Together, these data raise the question of the role of oxidative stress in regenerative neurogenesis in zebrafish.

KEYWORDS

brain injury, immune cells, microglia, neurogenesis, oxidative stress, SOD, teleost

1 | INTRODUCTION

Microglia were discovered in the early 1920 by Pío del Río Hortega and are derived from progenitors present in the embryonic yolk sac (Ginhoux et al., 2013; Sierra et al., 2016). They are macrophage-like cells located in the central nervous system, representing about 10–20% of glial cells (Nayak et al., 2014; Var & Byrd-Jacobs, 2020). Microglial cells exhibit a very important plasticity and are capable of major adaptations through structural and functional modifications. Under physiological conditions, most microglia remain in a quiescent state with a small cell body and highly branched processes, allowing immediate sensing of the microenvironment. In contrast, under pathological conditions (i.e., degenerative diseases, strokes, brain injuries, and infections), microglial cells rapidly adopt a phagocytic, amoeboid, and mobile phenotype, allowing them to move and reach the damaged area (Stence et al., 2001). During brain injury, microglia participate in the removal of cell debris and constitute key players of neuroinflammatory and oxidative stress processes (Fischer & Maier, 2015; Kim & Joh, 2006; Simpson & Oliver, 2020; Smith et al., 2012).

Due to its strong neurogenic activity and capacity to repair large brain injuries, zebrafish is emerging as an excellent model to study brain plasticity and regeneration (Alunni & Bally-Cuif, 2016; Diotel et al., 2013; Diotel et al., 2020; Ghaddar, Lubke, et al., 2021; Kishimoto et al., 2012; März et al., 2011; Schmidt et al., 2014; Zambusi & Ninkovic, 2020). As a result, a growing number of studies have begun to examine the role of neurotrophic factors such as brain-derived neurotrophic factor, nerve growth factor, and neurotrophins in brain repair conditions (Anand & Mondal, 2018, 2020; Cacialli et al., 2018; Bhattarai et al., 2020; Cacialli, 2021). Similarly, special attention has been paid to the research on microglia/immune cells, neuroinflammation, and oxidative stress in brain injury and neurodegenerative conditions in zebrafish (Kyritsis et al., 2012; Bhattarai et al., 2017; Kanagaraj et al., 2020; Var & Byrd-Jacobs, 2020). As in mammals, zebrafish microglia represent the major neuroinflammatory cells from the brain and can dynamically change their phenotype depending on the physiological context. After brain damage, they are activated and recruited to the damaged area (Kroehne et al., 2011; März et al., 2011; Baumgart et al., 2012; Kyritsis et al., 2012; Casano et al., 2016; Silva et al., 2020; Ghaddar et al., 2021). Moreover, after traumatic brain injury in mammals, peripheral immune cells can enter and remain transiently within the central nervous system, with some differentiating into resident microglia (Alam et al., 2020). Thus, after telencephalic injury in zebrafish, an acute inflammation occurs associated with abundant pro-inflammatory cytokine release, intense microglia activation, and potent peripheral immune cell infiltration (Kyritsis et al., 2012). This inflammatory state has been shown to be essential for the brain repair process and its inhibition resulted in decreased regenerative neurogenesis (Kyritsis et al., 2012). Moreover, the inhibition of microglia activation in zebrafish led to impaired regeneration as described recently in a preprint study (Kanagaraj et al., 2020). Taken together, these data argue for a role of microglia/immune cells and inflammation in brain repair mechanisms.

The cellular damage and death that occur during injury also lead to mitochondrial dysfunction and the excessive production of reac-

tive oxygen species (ROS), including the superoxide anion radical, hydroxyl radical, and hydrogen peroxide (H_2O_2). The resulting imbalance between free radicals and antioxidant defenses induces the generation of oxidative stress. In order to maintain homeostasis, several antioxidant defenses are activated. They involve among others the enzymes superoxide dismutase (SOD), catalase, and glutathione peroxidase (GPx). SODs are the first detoxification enzymes and catalyze the dismutation of two superoxide anion molecules into H_2O_2 and molecular oxygen. Then, catalase reduces H_2O_2 to water and molecular oxygen, thus completing the detoxification process initiated by SOD. Similarly, GPx breaks down H_2O_2 into water. In parallel, glutathione reductase reduces glutathione disulfide to the sulfhydryl form of glutathione, thus helping to resist oxidative stress. Together, these different enzymatic activities help restore redox balance within the tissue. While the characterization of antioxidant defenses is well described in mammals during injury (Lin et al., 2021; Praveen Kumar et al., 2021), very few data are available in zebrafish. Nevertheless, the recent work from Anand et al. (2021) demonstrated that antioxidant enzyme activity was modulated after zebrafish brain injury in links with increased levels of lipid peroxidation and GSH (reduced glutathione).

In this study, we set out to provide a better general overview of the distribution of microglia in the adult zebrafish brain, highlighting their intimate links to blood vessels and neurogenic niches. Given the emerging roles of microglia in brain regeneration (Bhattarai et al., 2016; Diaz-Aparicio et al., 2020), we took advantage of a recently published RNA-sequencing (RNAseq) dataset on the telencephalon of stab-wounded adult zebrafish to reanalyze the expression of important microglial genes (Rodriguez Viales et al., 2015; Gourain et al., 2021). Thus, we correlate the overexpression of microglia markers at 5 days post-lesion (dpi) with gene expression and activities of oxidative stress mediators.

2 | MATERIALS AND METHODS

2.1 | Animals and ethics

Three-to-six-month-old adult zebrafish, wild type, *Tg(mpeg1.1:mCherry)*, *Tg(mpeg1.1:GFP)*, double transgenic *Tg(mpeg1.1:mCherry) × Tg(GFAP::GFP)*, and *Tg(mpeg1.1:mCherry) × Tg(fli:GFP)* were housed at the CYROI/DéTROI zebrafish facility and maintained under standard conditions (28.5°C; 14-h dark/10-h light, pH 7.4, and conductivity at 400 μ S). All experiments were conducted in zebrafish in accordance with the French and European Community guidelines for the use of animals in research (86/609/EEC and 2010/63/EU) and approved by the local CYROI animal experimentation ethics committee and the French government (APAFIS 2018040507397248 v2).

2.2 | Stab wound injury of the telencephalon

To perform the telencephalic lesion, fish were deeply anesthetized with 0.02% tricaine (MS-222; REF: A5040, Sigma-Aldrich) and a sterile needle (BD Microlance 3; 30G \times 0.5 in.; 0.3 \times 13 mm²) was inserted into the right telencephalic hemisphere as previously described (März

et al., 2011; Diotel et al., 2013; Rodriguez Viales et al., 2015; Dorsemans, Soule, et al., 2017). At 5 dpl, fish were sacrificed and processed for immunohistochemistry or protein extraction from control and injured hemispheres.

2.3 | Tissue preparation

Fish were euthanized with tricaine before being fixed overnight at 4°C in 4% PFA (paraformaldehyde) dissolved in 1× PBS (Phosphate Saline Buffer). The next day, zebrafish were dissected and the brains were extracted and dehydrated in 100% methanol before being stored at −20°C until use.

2.4 | Immunohistochemistry (IHC) and TUNEL staining

For immunohistochemistry, brains were processed as described previously (März et al., 2011; Dorsemans, Lefebvre d'Hellencourt, et al., 2017; Ghaddar, Bringart, et al., 2021). Briefly, brains were rehydrated and permeabilized with PTw (1× PBS containing 0.1% Tween), embedded in 2% agarose, and sectioned (50 µm thickness) using a vibratome (VT1000S, Leica). After 1 h of blocking in PTw containing 0.2% BSA and 1% DMSO, the sections were incubated with the respective antibodies such as anti-Lcp1/L-plastin (rabbit anti-L-plastin from zebrafish, kindly provided by Dr. Michael Redd; 1/10,000) and anti-PCNA (proliferative cell nuclear antigen) (DAKO, clone PC10; Reference: M087901; 1/500) overnight at 4°C.

The next day, the sections were washed 3 times with PTw and incubated with the respective antibodies: Alexa Fluor® 488 goat anti-mouse antibody (ThermoFisher, Reference: A-11001; 1/500), Alexa Fluor® 594 goat anti-rabbit antibody (ThermoFisher, Reference: A-11012; 1/500) and/or with Alexa fluor 594-coupled anti-mCherry antibody (ThermoFisher, Reference: M11240; 1/500) or Alexa fluor 488-coupled anti-GFP (ThermoFisher, Reference: A-21311; 1/500) for 2 h at room temperature (RT). During this time, counterstaining of cell nuclei with DAPI was also performed. Finally, the sections were washed with PTw and mounted on slides with Aqua-Poly/Mount (Polysciences).

Note that each immunohistochemistry experiment was performed on at least three different animals in independent experiments. The antibodies are listed in Table 1.

For cell death quantification, TUNEL staining was performed using an In Situ Cell Death Detection Kit, TMR red (Roche; Reference: 12 156 792 910) following manufacturer's instructions. Quantification has been done on four brains.

2.5 | DCFH-DA staining and cell dissociation

To analyze oxidative stress after brain injury, an intraperitoneal injection of DCFH-DA was performed in anesthetized zebrafish. After 30 min, fish were stabbed in the right telencephalic hemisphere and allowed to recover for 30 min. Finally, they were fixed in 4% PFA and processed for microscopic analysis.

To investigate the nature of cells showing oxidative stress at 5 days, stab wounds were inflicted on *Tg(mpeg1.1:mCherry)* fish, which then survived for 5 days. Then, fish were sacrificed and brain cell dissociation was performed. Briefly, three injured telencephala were dissected, pooled, and recovered with PBS. They were then treated with PBS containing 0.1% trypsin and 1 mM EDTA and incubated at 28°C for 15 min by pipetting every 2 min. After 7 min of incubation, DCFH-DA was added (25 µM). Finally, centrifugation (1000 g, 4 min at 4°C) was performed and the cell pellet was resuspended in PBS containing DAPI for nuclear staining before microscopic observations.

2.6 | Protein extraction for cerebral antioxidant activities

At 5 dpl, fish were euthanized and the skull was immediately open in order to separate and remove the control and injured telencephalon. Three pools of five control telencephala and three pools of five injured telencephala were collected and snapped frozen. This experiment was reproduced 2 times independently.

To determine the SOD and peroxidase activities, protein isolation from 5 dpl control and injured hemispheres was performed as follows. Four-to-eight milligram of zebrafish hemispheres were collected and stored at −80°C before being homogenized with a TissueLyser II (QIAGEN) in 100 µl of Tris buffer (Tris [25 mM], EDTA [1 mM], NaCl [50 mM], and pH 7.4). After centrifugation (5000 rpm, 4°C for 10 min), the supernatant was used for protein quantification and enzymatic assays. Total proteins of lysate were quantified by the bicinchoninic acid assay.

Total SOD activity was determined using the cytochrome c reduction assay, as previously described (Dobi et al., 2019). Superoxide radicals generated by the xanthine/xanthine oxidase system reduce the ferricytochrome c into ferrocyanochrome c, thereby leading to an increase in absorbance at 560 nm. A 10 µl aliquot (about 30 µg of protein) of the lysates was combined with 170 µl reaction mixture (xanthine oxidase, xanthine [0.5 mM], cytochrome c [0.2 mM], KH₂PO₄ [50 mM, pH 7.8], EDTA [2 mM], and NaCN [1 mM]). The reaction was monitored in a microplate reader (FLUOstar OPTIMA, BMG Labtech, France) at 560 nm for 1 min, at 25°C. Total SOD activity was calculated using a calibration standard curve of SOD (up to 6 units/mg). Results were expressed as international catalytic units per microgram of cell protein, and peroxidase activities of telencephalic hemisphere lysates were assessed according to the protocol described by Everse et al. (1994). A reaction mixture was prepared with 200 µl of 50 mM citrate buffer/0.2% o-dianisidine and 5 µl of lysates (between 15 and 20 µg of protein). The reaction was initiated by adding 20 µl of 200 mM H₂O₂. Peroxidase activity was determined by measuring the absorbance at 450 nm at 25°C for 3 min. Peroxidase activity was expressed as international catalytic units per µg of proteins.

The determination of extracellular H₂O₂ production was performed by using *N*-acetyl-3,7-dihydroxyphenoxazine (Amplex Red) reagent. In the presence of horseradish peroxidase (HRP), this highly sensitive and stable probe reacts with H₂O₂ to produce highly fluorescent resorufin (Rhee et al., 2010). Lysates (10 µl/30 µg of protein) were incubated in 96-well plates with the reaction buffer (50 µl) (Amplex Red 100 mM,

TABLE 1 Antibodies

Antibodies	Interest	Host	Reference	Dilution	RRID
PCNA (proliferative cell nuclear antigen)	Cell proliferation	Mouse	DAKO, clone PC10; Reference: M087901	1/500	RRID:AB 2160651
Lcp1 (L-plastin) (lymphocyte cytosolic protein 1)	Microglia	Rabbit	Kindly provided by Dr. Michael Redd	10,000	Not provided (Redd et al., 2006)
Alexa Fluor® 488 goat anti-mouse antibody	PCNA antibody detection	Goat	ThermoFischer A-11001	1/500	RRID:AB 2534069
Alexa Fluor® 594 goat anti-rabbit antibody	LCP1 antibody detection	Goat	ThermoFischer A-11012	1/500	RRID:AB 141359
Anti-mCherry coupled to Alexa fluor 594	Boost mCherry labeling	Rat	ThermoFisher, M11240	1/500	RRID:AB 2536614
Anti-GFP coupled to Alexa fluor 488	Boost GFP labeling	Rabbit	ThermoFisher, A-21311	1/500	RRID:AB 221477

HRP 1 U/ml in Tris-HCl 50 mM, pH 7.4) for 30 min at RT. The fluorescence intensity was measured with excitation/emission wavelength set at 550/590 nm. Hydrogen peroxide production content was calculated using a calibration standard curve of H₂O₂ (ranged from 4 to 40 nM) and was expressed as nM of H₂O₂ per µg of proteins.

2.7 | RNA-sequencing data set analyses

For RNAseq analyses, data were reanalyzed from the Rodriguez Viales et al. (2015) and Gourain et al. (2021) studies for control and injured telencephalon (5 dpl; $n = 3$).

2.8 | Microscopy

Micrographs were obtained with an Eclipse confocal (Nikon) and with an AXIO OBSERVER 7 equipped with the Apotome.2 (Zeiss). The brightness and contrast of the images were adjusted in Adobe Photoshop.

2.9 | Cell counting

To determine the number of microglia and proliferating cells, the total area of mpeg- and PCNA-positive cells was measured on a 50-µm-thick vibratome cross section through the core of the lesion. Quantification was done using ImageJ software on a total of three fish. Comparisons between control and injured hemisphere were done on a total of three fish performing a student *t* test. Values were considered as significantly different when *p*-values < 0.05.

2.10 | Microglia density assessment

To investigate the relative abundance of microglia, at least three brains were analyzed in different respective regions and visually estimated and/or counted for Table 2 and Figure 3. A relative scale was proposed

as “/”: not detected; “+/-”: very few microglia; “+”: some microglia; “++”: abundant microglia; “+++”: very abundant microglia. This relative abundance quantification was verified by another round of quantification reinforcing the first results obtained. In addition, in some regions, a manual cell counting was performed to generate Figure 3.

2.11 | Nomenclature and abbreviations

The nomenclatures correspond to those provided in the zebrafish brain atlas (Wullimann et al., 1996). The schemes were modified and adapted from Wullimann et al. (1996) and Menuet et al. (2005). A, anterior thalamic nucleus; APN, accessory pretectal nucleus; ATN, anterior tuberal nucleus; CCe, corpus cerebelli; Chab, habenular commissure; Chor, horizontal commissure; CM, corpus mamillare; CP, central posterior thalamic nucleus; CPN, central pretectal nucleus; Cpop, postoptic commissure; Cpost, posterior commissure; D, dorsal telencephalic area; Dc, central zone of dorsal telencephalic area; DI, lateral zone of dorsal telencephalic area; Dm, medial zone of dorsal telencephalic area; DOT, dorsomedial optic tract; Dp, posterior zone of dorsal telencephalic area; DP, dorsal posterior thalamic nucleus; ECL, external cellular layer of olfactory bulb; EG, eminentia granularis; ENv, entopeduncular nucleus, ventral part; FR, fasciculus retroflexus; GL, glomerular layer of olfactory bulb; Had, dorsal habenular nucleus; Hav, ventral habenular nucleus; Hc, caudal zone of periventricular hypothalamus; Hd, dorsal zone of periventricular hypothalamus; Hv, ventral zone of periventricular hypothalamus; ICL, internal cellular layer of olfactory bulb; IL, inferior lobe; LH, lateral hypothalamic nucleus; LLF: lateral longitudinal fascicle; LR, lateral recess of diencephalic nucleus; MLF, medial longitudinal fascicle; NMLF, nucleus of medial longitudinal fascicle; PG, preglomerular nucleus; PGa, anterior preglomerular nucleus; PGI, lateral preglomerular nucleus; Pit, pituitary; PO, posterior pretectal nucleus; PP, periventricular pretectal nucleus; PPa, parvocellular preoptic nucleus, anterior part; Ppp, parvocellular preoptic nucleus, posterior part; PR, posterior recess of diencephalic ventricle; PSp, parvocellular superficial pretectal nucleus; PTN, posterior tuberal nucleus; R, rostralateral nucleus; RF, reticular formation; SC, suprachiasmatic

TABLE 2 Relative microglia density in the different brain regions

Regions	Relative density
Olfactory bulbs	+
Ventral telencephalic area (subpallium parenchyma)	+
Dorsal part (Vd)	+
Ventral part (Vv)	+
Central nuclei (Vc)	+/-
Supracommissural nuclei (Vs)	+
Postcommissural nuclei (Vp)	+
Area dorsalis telencephali (pallium parenchyma)	+
Central zone of D (Dc)	+
Lateral zone of D (DI)	+
Medial zone of D (Dm)	+
Posterior zone of D (Dp)	+/-
Preoptic diencephalic region (parenchyma)	+
Anterior parvocellular preoptic nucleus (PPa)	+
Posterior parvocellular preoptic nucleus (PPp)	+
Suprachiasmatic nucleus (SC)	+/-
Thalamus	++
Anterior nucleus (A)	++
Dorsal posterior thalamic nuclei (DP)	
Central posterior thalamic nuclei (CP)	
Ventromedial nuclei (VM)	++
Ventrolateral nuclei (VL)	++
Caudal thalamus posterior tuberculum (parenchyma)	++
Periventricular nucleus of the posterior tuberculum (TPp)	+
Posterior tuberal nucleus (PTN)	+/-
Torus lateralis (TLa)	+
Hypothalamus (parenchyma)	++
Ventral zone of the periventricular nucleus (Hv)	+/-
Anterior tuberal nucleus (ATN)	+/-
Lateral hypothalamic nucleus (LH)	+/-
Cells surrounding laterocaudal ventricular recesses (LR)	+
Cells surrounding posterior ventricular recesses (PR)	+
Caudal zone of the periventricular hypothalamus (Hc)	++
Dorsal zone of periventricular hypothalamus (Hd)	+/-
Inferior lobe (IL)	+
Mesencephalon (parenchyma)	+++
Tectum opticum (TeO)	+
Torus longitudinal (TL)	/
Torus semicircularis (TS)	+++
Cerebellum (VCe+Ce)	+

Note: The analysis of the relative abundance/density of microglia was performed by visual observation of brain sections. The analysis was done according to this legend: “/”: not detected; “+/-”: very few microglia. “+”: some microglia. “++”: abundant microglia; “+++”: very abundant microglia. Note that microglia are found in almost all the brain regions.

nucleus; SD, saccus dorsalis; SO, secondary octaval population; TeO, tectum opticum; TL, torus longitudinalis; TLa, torus lateralis; TPp, periventricular nucleus of posterior tuberculum; TS, torus semicircularis; V, ventral telencephalic area; V3, third ventricle; VII, sensory root of the facial nerve; VIII, octaval nerve; VCe, valvula cerebelli; Vd, dorsal nucleus of ventral telencephalic area; VL, ventrolateral thalamic nucleus; VM, ventromedial thalamic nucleus; VOT, ventrolateral optic tract; Vp, postcommissural nucleus of ventral telencephalic area; Vv, ventral nucleus of ventral telencephalic area; ZL, zona limitans.

3 | RESULTS

3.1 | Distribution and morphology of L-plastin and mpeg1.1-positive cells (microglia) in the adult zebrafish brain under homeostatic conditions

We first decided to provide a general overview of the distribution of microglia in the adult zebrafish brain. For this purpose, we used the Tg(*mpeg1.1:GFP*) transgenic fish line (labeling microglia in the brain) and performed L-plastin (Lcp1) immunohistochemistry considering that under homeostatic condition, no peripheral immune cell infiltration occurs. We first demonstrated that both markers (*mpeg1.1* and L-plastin) were highly co-expressed in microglial cells within different brain regions such as the telencephalon and the mesencephalon parenchyma (Figure 1). In the healthy brain, we observed elongated, ramified, and rounded/amoeboid cells throughout all the regions studied (Figure 1, left panels). Evidently, in the midbrain, microglia appeared much more ramified/hyper-ramified than in the telencephalon, as shown in Figure 1 (right panels). The different morphologies were also shown in Figure S1.

In the forebrain, we observed a few microglial cells in the periphery and interior of the olfactory bulbs by performing L-plastin immunohistochemistry (not shown). In the telencephalon, small numbers of microglia were detected in all nuclei and brain regions, including the central (Dc), dorsomedian (Dm), and dorsoposterior (Dp) regions of the pallium as well as the central (Vc), ventral (Vv), and dorsal (Vd) nuclei of the subpallium. Microglia were detected in the brain parenchyma and also in close proximity to the ventricles (Figure 2a).

More dorsally, microglia were again detected in the pallium, particularly in the dorsolateral telencephalon (DI). They were also reported in the postcommissural nucleus of the ventral telencephalic area (Vp) (Figure 2b). In the diencephalon, a high density of microglia was observed in the anterior (PPa) and posterior (PPp) parts of the preoptic area, in the entopeduncular nucleus (Env), suprachiasmatic nucleus (SC), ventrolateral and ventromedial thalamic nuclei (VL and VM, respectively), and in the habenula (Hav) (Figure 2b,c). Overall, our data showed that in the forebrain, under homeostatic conditions, microglia appear to be elongated or rounded but not so hyper-ramified.

More caudally, numerous and abundant microglia were detected in the ventral, mediobasal, and caudal hypothalamus (Figure 2d-f) along the ventricular layer but also in the parenchyma. A significant number of microglia were detected along the lateral and posterior recess of the hypothalamus. They were also observed in the optic tectum (TeO),

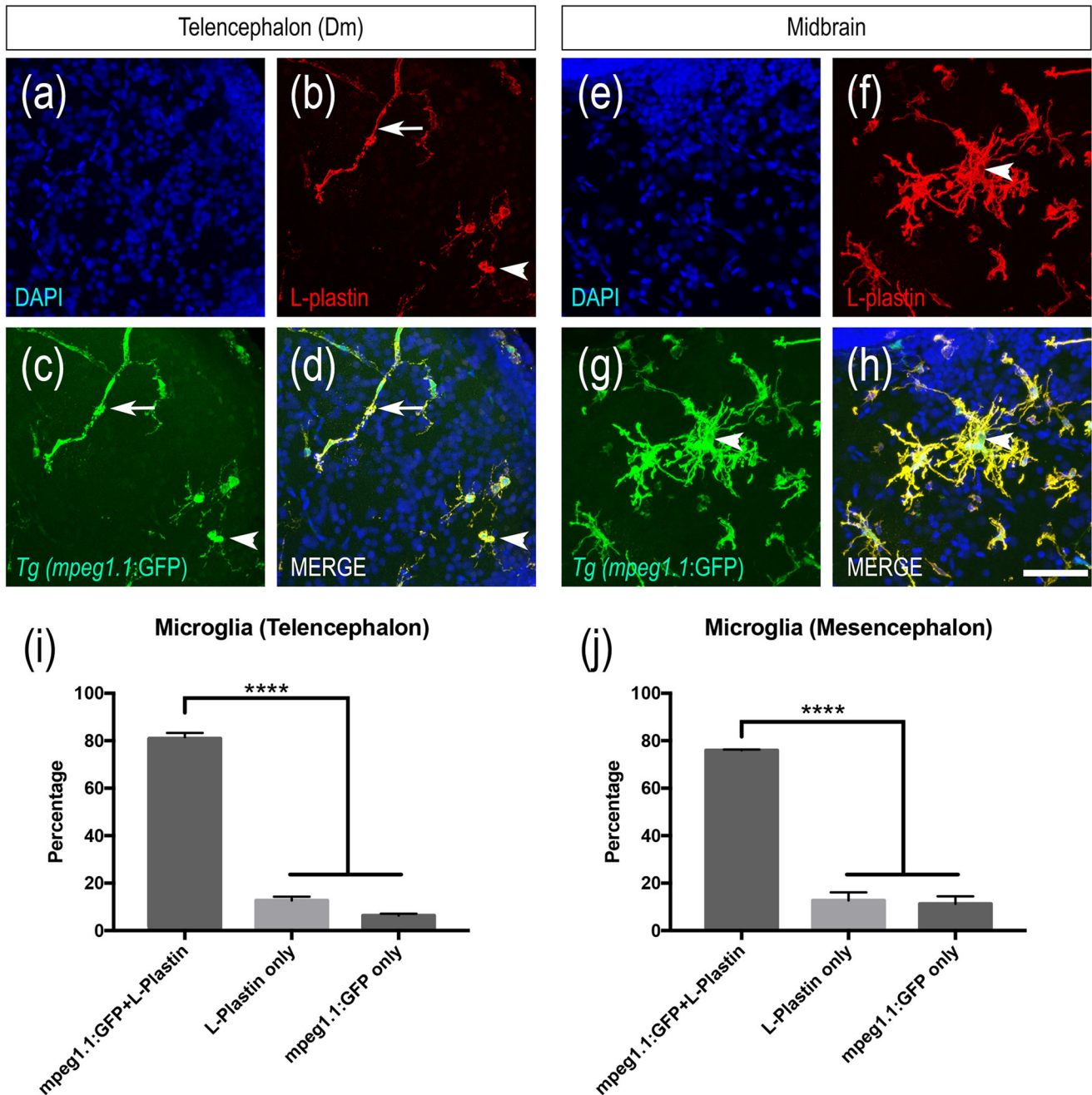


FIGURE 1 Co-expression of L-plastin and mpeg1.1:GFP in microglia from the telencephalon and midbrain regions showing different microglia morphologies. (a–h) L-Plastin immunohistochemistry (red, b and f) on *Tg(mpeg1.1:GFP)* fish (green, c and g) with DAPI counterstaining (blue, a and e) showing a co-expression of both markers in the dorsomedian (Dm) telencephalon (left panels) and the midbrain parenchyma (right panels). In the telencephalon, most microglia appeared elongated (arrows) or rounded with a low number of processes (arrowheads). In contrast, in the posterior part of the brain, microglia appeared hyper-ramified (arrowheads). Bar: 70 μ m. (i and j) Quantification of the number of mpeg1.1:GFP and L-plastin double positive cells, L-plastin-positive cells only, and mpeg1.1:GFP positive cells only in the central telencephalon and mesencephalon. Note that most of microglial cells express both markers. $n = 3$ brains; **** $p < 0.0001$

the torus longitudinalis (TLa), the anterior preglomerular nucleus (Pga), and in the cerebellum, especially in the valvula cerebelli (VCe). L-Plastin-positive cells were also found in the periventricular nucleus of the posterior tubercle (TPp) and in the zona limitans (ZL). A high density of microglia was also observed below the TeO, near the tectal ventricle and in the region of the torus semicircularis (Ts). Clearly, microglia den-

sity appears to be higher in the hindbrain than in the telencephalon, and hyperbranched microglia are more numerous (Table 2 and Figure 3).

This distribution of microglia in the adult fish brain was also supported by the use of *Tg(mpeg1.1:mCherry)*. Therefore, under homeostatic conditions, we observed (1) elongated microglia that are notably localized in the telencephalon, (2) rounded/amoeboid

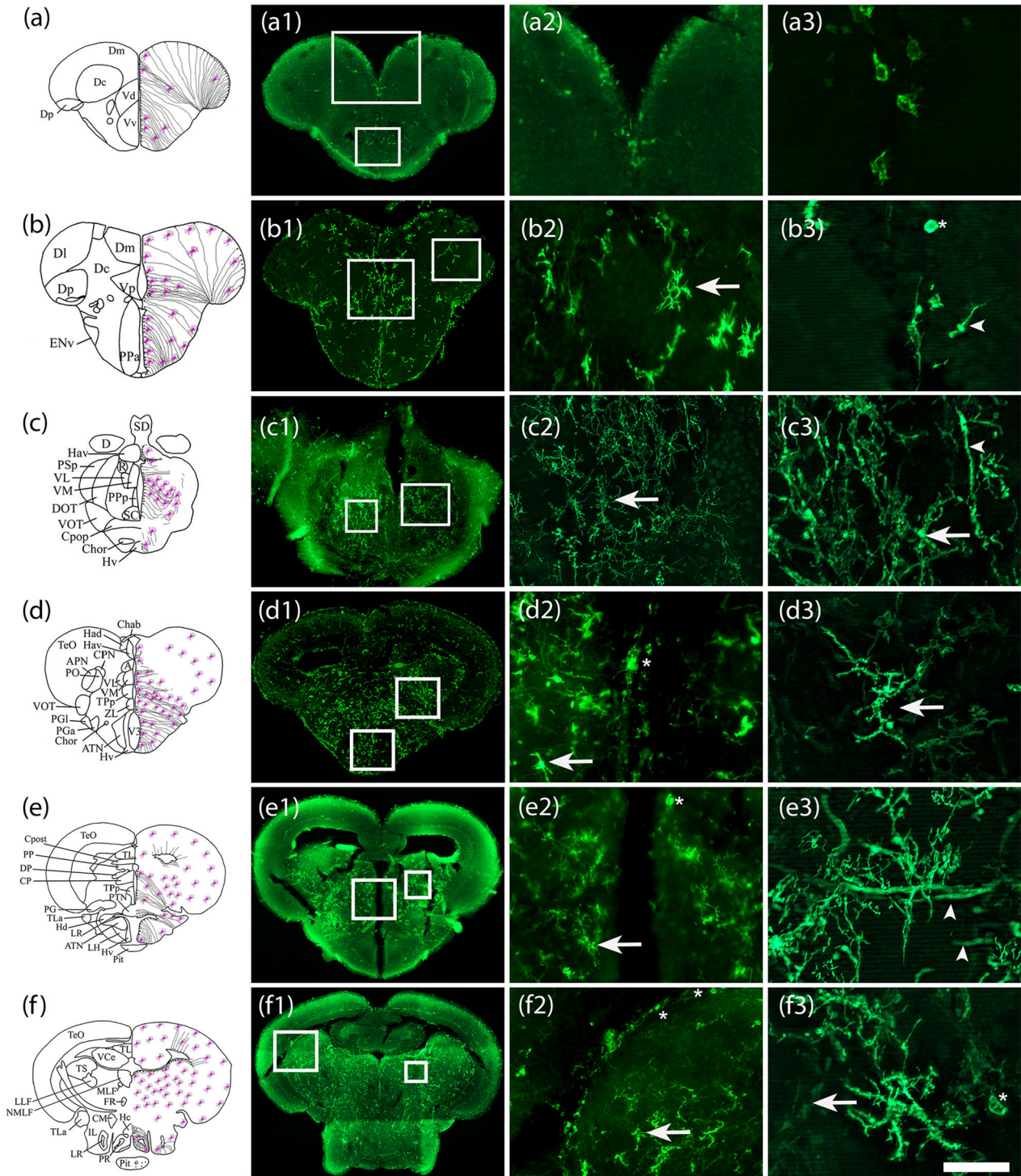


FIGURE 2 Mapping of microglia in the brain of adult zebrafish showing a heterogeneous distribution of microglia. (a–f) The scheme provides the localization of the transversal section with purple cells corresponding to the schematic distribution of microglia. (a–c) L-Plastin immunohistochemistry in the telencephalon (a and b), diencephalon with the anterior (b, PPa), and posterior (c, PPp) parts of the preoptic area. Note that in the telencephalon, ramified, elongated, and rounded microglia have been detected. (d–f) L-Plastin immunohistochemistry in transversal brain section through the anterior part of the hypothalamus (d, Hv), the mediobasal hypothalamus (e, Hv LR), and the caudal hypothalamus (at the level of LR PR). Note the higher density of microglia in the posterior brain section than in the telencephalon. Microglia were detected in the anterior part of the hypothalamus (d2), the periventricular nucleus of the posterior tuberculum (TPp in d3), the central posterior thalamic nucleus (CP in e2), the torus semicircularis (TS in f2), and midbrain parenchyma (f3). Note that the higher magnification pictures do not systematically correspond to the same picture of the lower magnification provided in (a1–f1). Arrows pointed to ramified microglia, arrowheads showed elongated microglia, and asterisks to almost amoeboid microglia. Bar: 30 μ m (a3, b2, b3; d2, d3, e3, and f3); 45 μ m (e2); 60 μ m (f2); 70 μ m (c3); 90 μ m (a2, c2); 200 μ m (c1); 500 μ m (d1, e1, and f1); 600 μ m (a1 and b1)

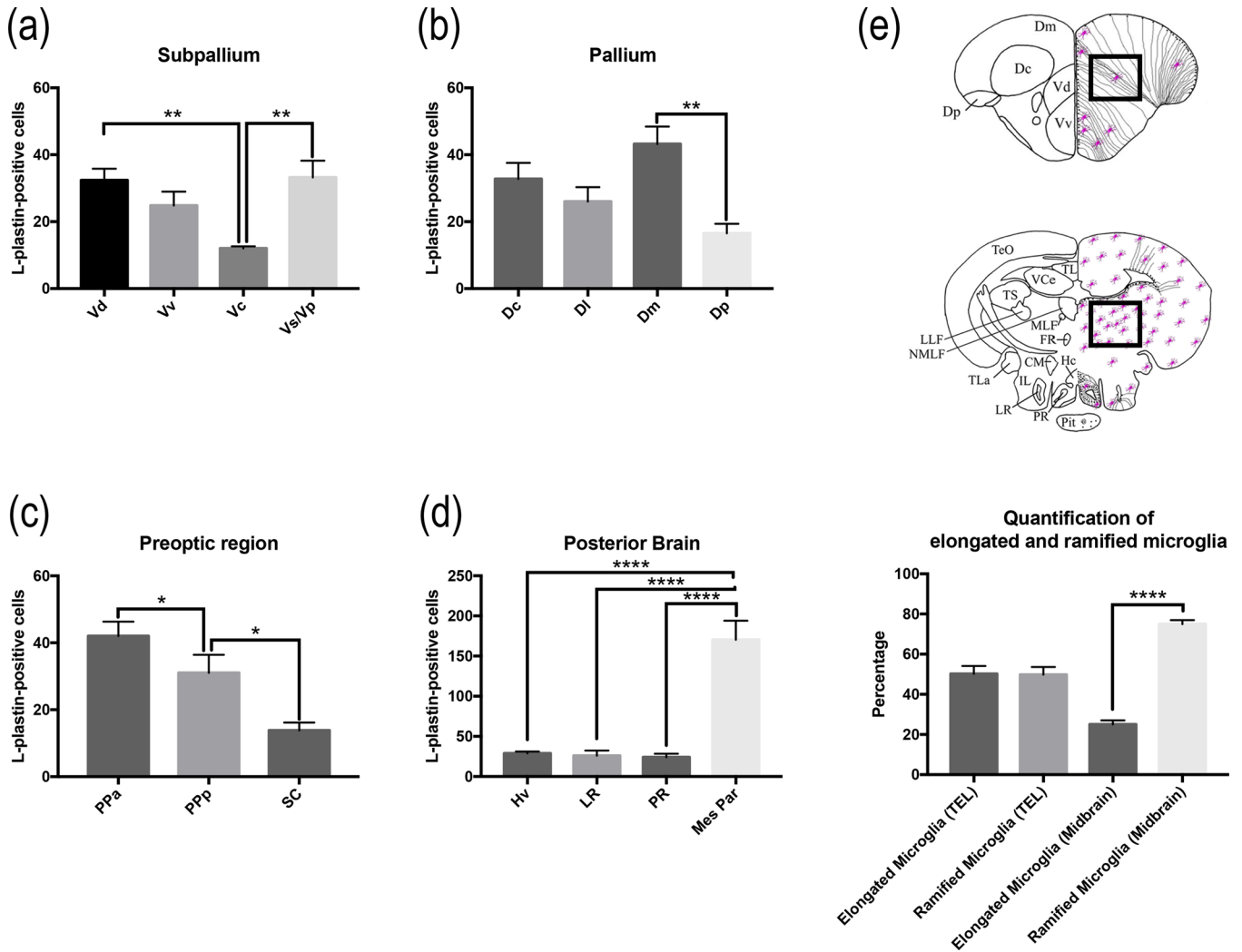


FIGURE 3 Number of L-plastin-positive cells in key regions of the adult zebrafish brain under homeostatic condition. (a–d) Graphs showing the number of L-plastin positive cells in the subpallium, pallium, preoptic region, and posterior brain (anterior hypothalamus, around the lateral and posterior recess, and in the midbrain parenchyma). Note that the number of L-plastin positive cells is higher in the midbrain parenchyma (Mes Par) compared to more anterior regions. (e) Percentage of elongated versus branched microglia analyzed in telencephalon (pallium) and midbrain parenchyma (Mes Par) as indicated by the black square in the upper schemes. Mes Par: Mesencephalon parenchyma. $n = 5$ brains; $*p < 0.05$; $**p < 0.01$; $****p < 0.0001$

microglia detected along all the ventricular layers from the tel-, di- and rhombencephalon as well as in the tela choroidea, and (3) ramified/hyper-ramified microglia. The latter microglia were more abundantly observed in the posterior part of the brain. These different morphologies were provided in Figure S1. The relative abundance of microglia within the different brain subdivision and brain nuclei/domains was provided in Table 2, Figures 3 and S2.

3.2 | Microglia are detected in the vicinity of blood vessels and neural stem cells (NSCs)

The careful observation of elongated microglia suggests that some microglia in zebrafish may also be associated with blood vessels. To confirm this hypothesis, we generated double transgenics by crossing

Tg(*mpeg1.1:mCherry*) with Tg(*fli:GFP*) fish, in which GFP is expressed in endothelial cells (Lawson & Weinstein, 2002; Cassam-Sulliman et al., 2021). As clearly demonstrated, many elongated microglial cells were extended along the blood vessels, namely, in the dorsolateral and dorsomedial telencephalon and in the preoptic area. In Figure 4c, microglia clearly surrounded a blood vessel (Figure 4c,f, arrow in high-power view).

In addition, numerous L-plastin and *mpeg1.1:mCherry*-positive cells were also detected in the ventricular/periventricular layer, where neural stem cells (NSCs) are located (Pellegrini et al., 2007; März et al., 2010). To better describe the potential interaction between microglia and NSCs, we generated double transgenic fish by crossing two existing lines and obtained Tg(*mpeg1.1:mCherry*) × Tg(*GFAP::GFP*) fish, allowing the detection of microglia and NSCs in red and green, respectively. In the pallium (Dm), we observed a close proximity of rounded/amoeboid

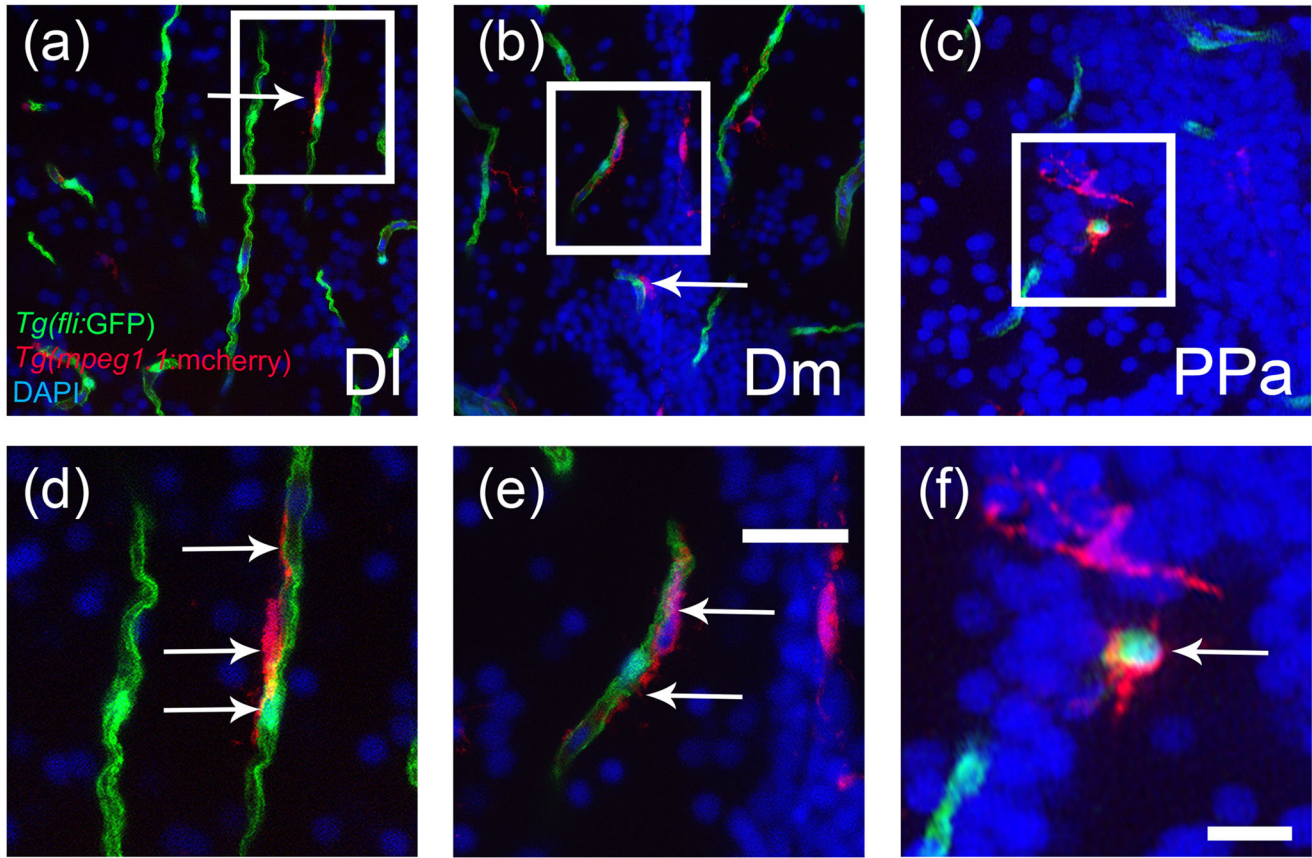


FIGURE 4 Microglia are detected along blood vessels in the brain. (a–f) Double transgenic *Tg(mpeg1.1:mCherry) × Tg(fli:GFP)* fish showing microglia (red) and endothelial cells (green), respectively. In the dorsolateral (DI) and dorsomedian (Dm) telencephalon, as well as in the anterior part of the preoptic area (PPa) of the diencephalon, numerous elongated microglia are interacting with blood vessels (arrows). (d–f) Higher magnifications of the respective white boxes found in (a–c). Note that such interactions were observed in the whole brain. Bar: 16 μm (f), 28 μm (d and e), 42 μm (c), and 70 μm (a and b)

microglia with GFAP::GFP positive NSCs (Figure 5a,d, arrows). Such interactions were also observed in the Vv/Vd (Figure 5b,e, arrows). Also, some microglia far from the ventricular zone also appeared to make contact with NSC processes as shown, for instance, in the posterior part of the preoptic area (PPp) (Figure 5f, arrows). Generally, these rounded/amoeboid cells were observed along the ventricular zones where NSCs are localized.

3.3 | Recruitment of microglia/peripheral immune cells during telencephalic regeneration and links to oxidative stress

After stab wound injury of the telencephalon, microglial cells are activated, then they proliferate and migrate to the injured site within few hours (März et al., 2011; Kyritsis et al., 2012; Ghaddar, Lubke, et al., 2021). In the injured hemisphere, the number of microglia increases to reach a peak between 2- and 3-day post-lesion according to the different studies, while their number remains constant in the control hemisphere (März et al., 2011; Kyritsis et al., 2012; Kanagaraj et al., 2020; Ghaddar, Lubke, et al., 2021). Moreover, it is well

admitted that after traumatic brain injuries, peripheral immune cells such as neutrophils and macrophages could be recruited to the damage area (Alam et al., 2020). In zebrafish, macrophages also express *mpeg1.1* and L-plastin. Consequently, in such traumatic conditions, the *mpeg1.1:mCherry* and L-plastin-positive cells could be microglia and peripheral immune cells.

In our study, we demonstrated using *Tg(mpeg1.1:mCherry)* that the number of microglia/immune cells was still significantly increased in the injured hemisphere at 5 dpl (Figure 6a,b). Similar results were also obtained by L-plastin immunohistochemistry (not shown). In parallel, a significant ventricular cell proliferation was observed in the lesioned hemisphere (Figure 6a,c), as previously described (Rodríguez Viales et al., 2015).

Reanalysis of the RNAseq data sets reinforced the immunostaining results. Indeed, focusing on the expression of six genes (*mpeg1.1*, *spi1a*, *slc7a7*, *irf8a*, *apoeb*, and *lcp1*) that were found to be enriched in zebrafish microglia (Oosterhof et al., 2017), we observed their significant upregulation 5 dpl (Figure 6d–i). Therefore, at 5 dpl, microglia are still activated and abundantly present in the injured hemisphere.

During brain damage, oxidative stress is an important factor occurring (Slemmer et al., 2008; Miyamoto et al., 2013; Hameed et al.,

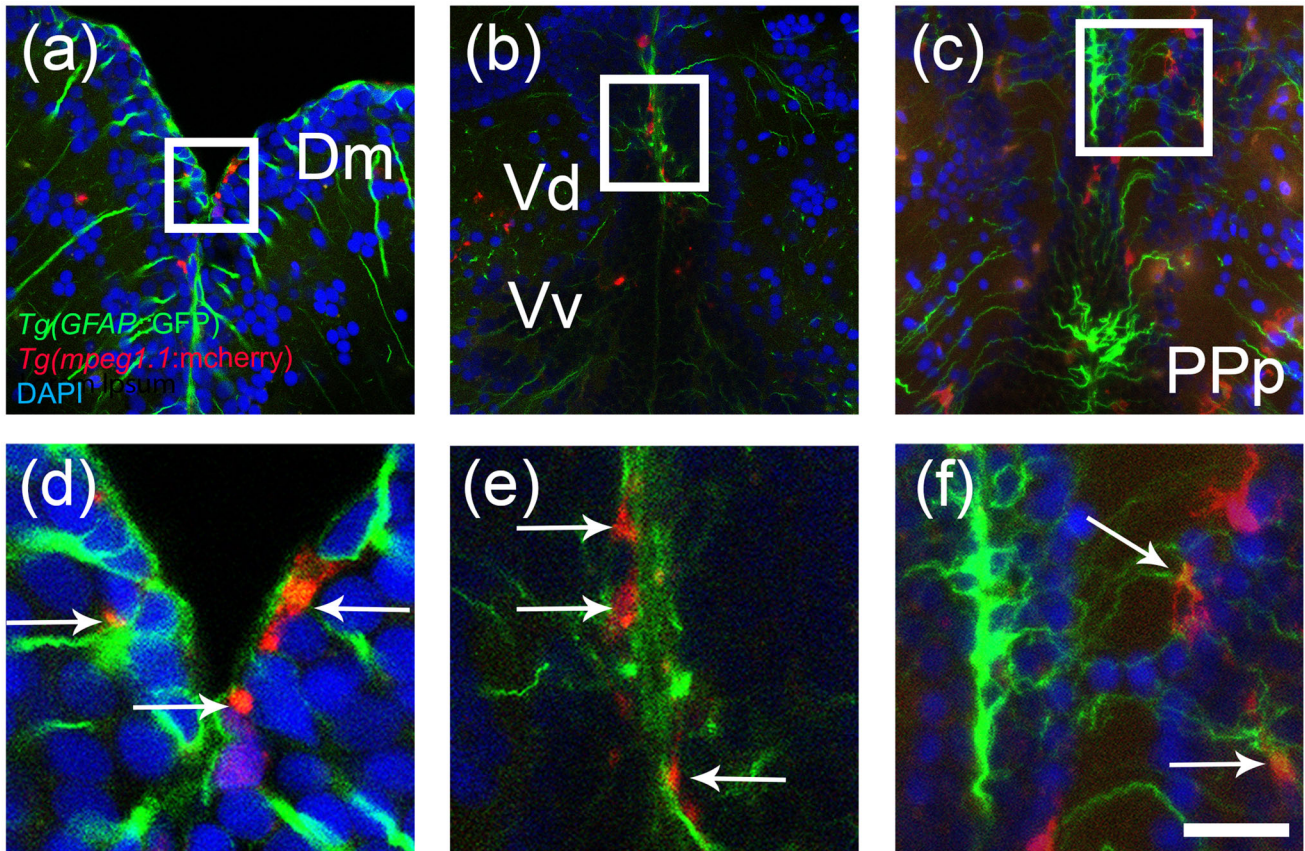


FIGURE 5 Some microglia are close to neural stem cells. (a–f) Double transgenic *Tg(mpeg1.1:mCherry) × Tg(GFAP::GFP)* fish showing microglia (red) and radial glial neural stem cells (radial glia in green), respectively. In the ventral (Vv and Vd nuclei) and dorsal (Dm) telencephalon as well as in the posterior part of the preoptic area (PPp) of the diencephalon, numerous rounded microglia are in the close vicinity of GFAP::GFP positive cells known to correspond to radial glia (neural stem cells) (arrows). Most of these interactions were observed at the ventricular surface (d and e) but also at the level of neural stem cell (NSC) processes in the parenchyma (f). (d–f) Higher magnifications of the respective white boxes found in (a–c). Bar: 14 μ m (d and e), 20 μ m (f), 40 μ m (a), and 60 μ m (b and c)

2015; Sakai & Shichita, 2019; Eastman et al., 2020). We consequently decided to use the DCFH-DA probe to monitor oxidative stress in our brain injury model. First, the efficiency of the probe was assessed in 3-day postfertilization elutheroembryos in a model of tail amputation well known to induce oxidative stress (Mugoni et al., 2014; Sipka et al., 2021). As expected, it led to DCFH-DA staining at the injury site (Figure 7a–c). So, we injected the DCFH-DA probe prior to telencephalic stab wound injury, and a strong fluorescent staining was observed 30 min after the lesion (Figure 7d). The telencephalic region where DCFH-DA staining was observed was also associated to cell death as shown by TUNEL staining (Figure 7e,f). In parallel, no DCFH-DA labeling was observed in 5 dpl hemisphere probably due to the inability of the probes to reach the brain tissue once brain repair had begun.

In mammals, ROS are generated by microglia via NADPH oxidase (NOX). Single-cell RNAseq demonstrated that *Nox2* (*Cybb*) is the most highly expressed *Nox* gene in human and mouse microglia (Zhang et al., 2014; Simpson & Oliver, 2020). In zebrafish, the *nox2* gene was also shown to be enriched in microglia, and Ingenuity Pathway Analysis showed that genes strongly expressed in microglia are notably associ-

ated with ROS production (Oosterhof et al., 2017). So far, we decided to monitor *nox2* gene expression by reanalyzing the RNAseq data set from Rodriguez Viales et al. (2015) and Gourain et al. (2021). *Nox2* expression was significantly upregulated in the injured hemisphere compared to the control one at 5 dpl (Figure 8a). Similarly, the expression of *nrf2a*, a transcription factor activated for combating oxidative stress, was also significantly increased at 5 dpl (Figure 8b).

At the same time, by performing the Amplex Red assay, we observed a significantly higher fluorescence in the injured hemisphere compared with the control. This shows that H_2O_2 levels are still elevated in the injured hemisphere 5 dpl (Figure 9c). Interestingly, cell dissociation from 5 dpl telencephalon and incubation with DCFH-DA demonstrated that numerous *mpeg1.1:mCherry* positive cells exhibited oxidative stress (Figure 9d, see arrows).

Given the presence of ROS and the upregulation of *nrf2*, known to regulate antioxidant defenses (Miller et al., 2012; Zhao et al., 2013), we then studied the gene expression of the main antioxidant enzymes GPx and SOD. The expression of *gpx1a* and *1b*, *gpx4a* and *4b*, and *gpx8* genes remained unchanged, whereas *gpx7* was significantly increased in the stab-wounded hemisphere (Figure 8d–f). The transcript level of

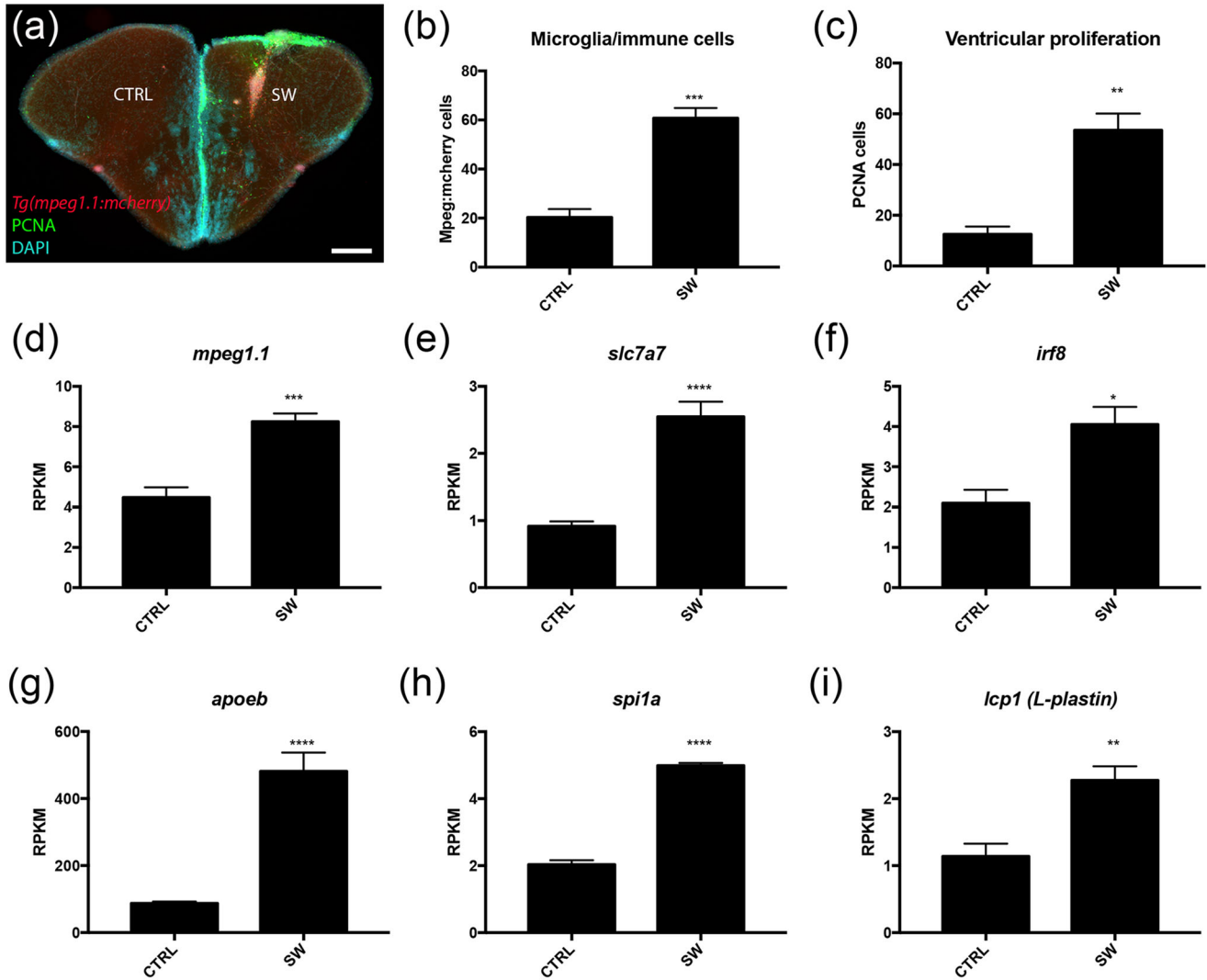


FIGURE 6 Recruitment of microglia/immune cells and expression of “microglia”-enriched genes at 5-day post-telencephalic injury. (a) Proliferative cell nuclear antigen (PCNA) immunohistochemistry (green) on Tg(mpeg1.1:mCherry) fish (red) showing a strong ventricular cell proliferation within the telencephalic neurogenic niche and the presence of a higher number of microglia 5 days after brain injury. (b and c) The quantification of the PCNA- and mpeg1.1:mCherry positive cells demonstrated their significant increase in the stab-wounded hemisphere (SW) compared to control one (CTRL). The quantification corresponds to the mean of three different brains. (d-i) Reanalysis of the RNA-sequencing data set from injured and uninjured zebrafish telencephalon at 5 dpl from Rodriguez Viales et al. (2015) and Gourain et al. (2021). Enriched microglia genes are upregulated at 5-day post-brain injury. * $p < 0.05$; ** $p < 0.01$; *** $p < 0.001$; **** $p < 0.0001$. Bar: 50 μm

sod1, *sod3a*, and *3b* remained unchanged at 5 dpl in the stab-wounded telencephalon compared to the control telencephalon, while *sod2* was barely but significantly reduced ($p = 0.03$). Interestingly, the *glutathione reductase* gene encoding the enzyme that reduces oxidized glutathione to the sulfhydryl form (reduced form) was significantly upregulated (Figure 8c). We also measured the activities of the antioxidant enzymes GPx and SOD. The SOD activity was significantly upregulated at 5 dpl. The GPx activity, which remains nonsignificant, was nevertheless observed to be increased in two independent experiments, correlated with a significant increase in Amplex Red staining (Figure 9b,c).

Taken together, these data suggest the persistence of a prooxidant environment up to 5 dpl and the activation of antioxidant defense,

associated with the presence of microglia and the activation of reactive neurogenesis. At 5 dpl, microglia seem to be an important contributor of oxidative stress generation.

4 | DISCUSSION

In this work, we provided a better description of the distribution of microglia in the adult zebrafish brain using immunohistochemistry of L-plastin and Tg(mpeg1.1:mCherry) fish in homeostatic conditions. Our results showed that microglia exhibited different distributions and phenotypes throughout the healthy brain. In addition, we also demonstrated a close association among microglia, blood vessels, and

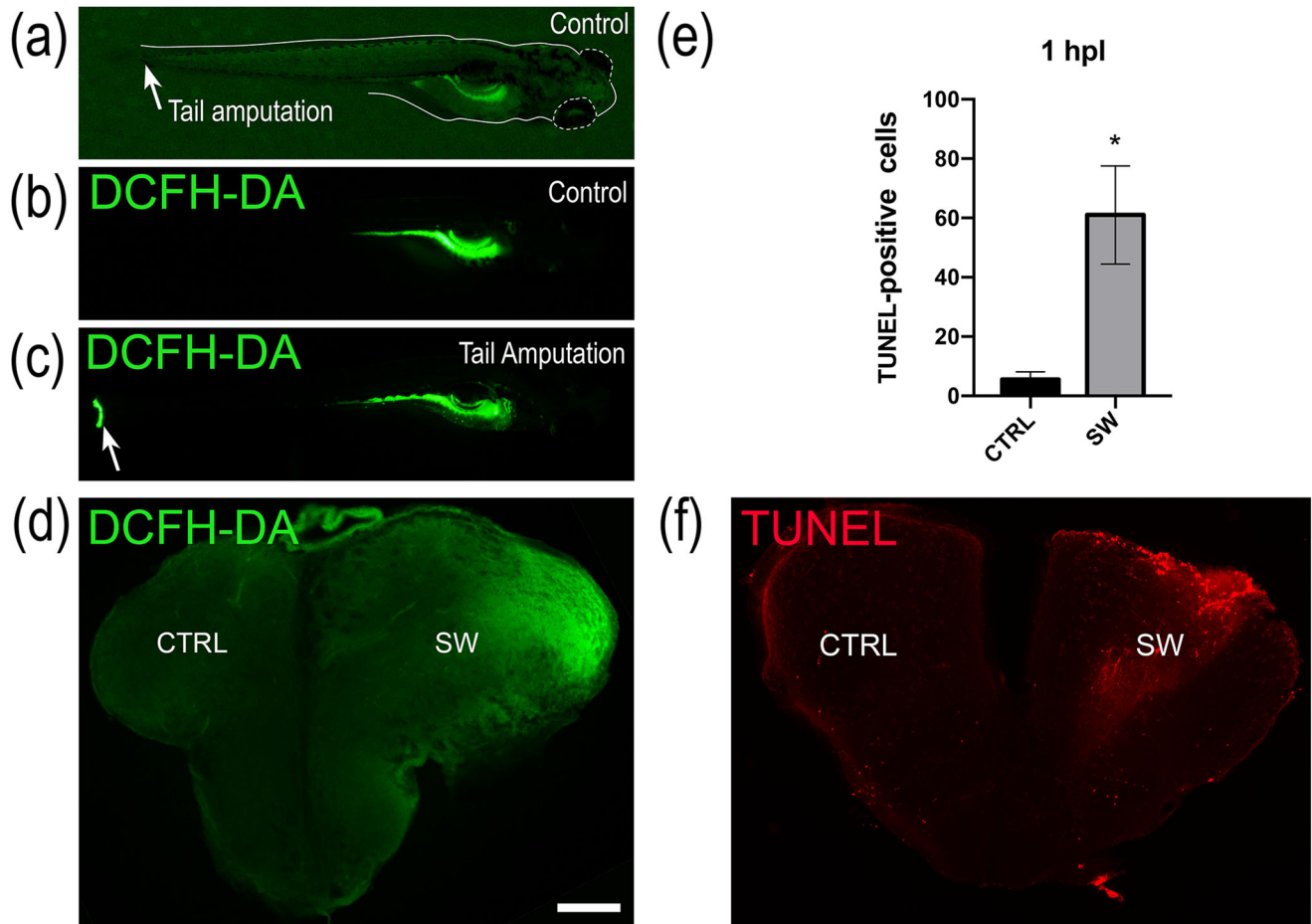


FIGURE 7 Brain injury leads to oxidative stress. (a) Representative picture of green autofluorescence in a 3-days postfertilization (dpf) eleutheroembryo following tail amputation. Note that no autofluorescence occurs at the injury site. (b) Representative DCFH-DA staining in a 3 dpf eleutheroembryo without tail amputation. No staining was observed at the injury site. (c) Representative DCFH-DA staining in a 3 dpf eleutheroembryo with tail amputation demonstrating the oxidative stress generated at the injury site (arrow). (d) Representative picture of DCFH-DA oxidative stress staining showing increased fluorescence in the stab-wounded hemisphere 30-min post-injury. (e and f) Quantification and representative picture of TUNEL-positive cells in the control (CTRL) and stab-wounded (SW) telencephalon at 1 h post-lesion ($n = 4$). Bar: 600 μm (a–c and f) and 50 μm (d); * $p < 0.05$

NSCs raising the question of a potent role for zebrafish microglia in the establishment and functions of the blood–brain barrier and in neurogenesis as shown in mammals. In the context of telencephalic injury, we noted that genes known to be enriched in microglia are still upregulated at 5 dpl (*mpeg1.1*, *slc7a7*, *irf8*, *apoeb*, *spi1a*, and *lcp1*). These data were also supported by an increased number of *mpeg1.1:mCherry*- and L-plastin-positive cells in the injured hemisphere compared with the control hemisphere. Furthermore, we showed that some important regulators of oxidative stress are also upregulated at 5 dpl, such as *nox2*, *nrf2a*, and *glutathione reductase*, while gene expression of antioxidant enzymes (SOD and GPX) remains almost unchanged, except for *gpx7* and *sod2* that were slightly increased and decreased, respectively. However, SOD activity was significantly higher in the injured telencephalon, correlated to an increase in H_2O_2 levels without significant change in peroxidase activity. Together, these data highlight the distribution and potent functions of microglia/immune cells in brain homeostasis in constitutive and regenerative conditions and suggest important roles of oxidative stress in brain regeneration.

4.1 | Microglia are widely but heterogeneously distributed in the brain of adult zebrafish

In our study, we provided a detailed mapping of microglia distribution across the different brain nuclei and domains of adult zebrafish based on L-plastin immunohistochemistry and using *Tg(mpeg1.1:mCherry)* fish. This general overview of microglia distribution in the brain of adult zebrafish completed other studies that mainly focused on some brain regions such as some telencephalic and midbrain areas (März et al., 2011; Baumgart et al., 2012; Oosterhof et al., 2018; Wu et al., 2020; Cassam-Sulliman et al., 2021). We observed microglia in all brain subdivisions studied (tel-, di-, rhombencephalon). Interestingly, we noticed that the density of microglia varies from one brain regions to another, as well as its morphology. For example, in the telencephalon, the density of microglia under homeostatic conditions is quite low, whereas it is much higher in the mesencephalon (in the optic tectum and the brain domains below). These data raise the question of the roles and mechanisms that support the correct establishment of microglia

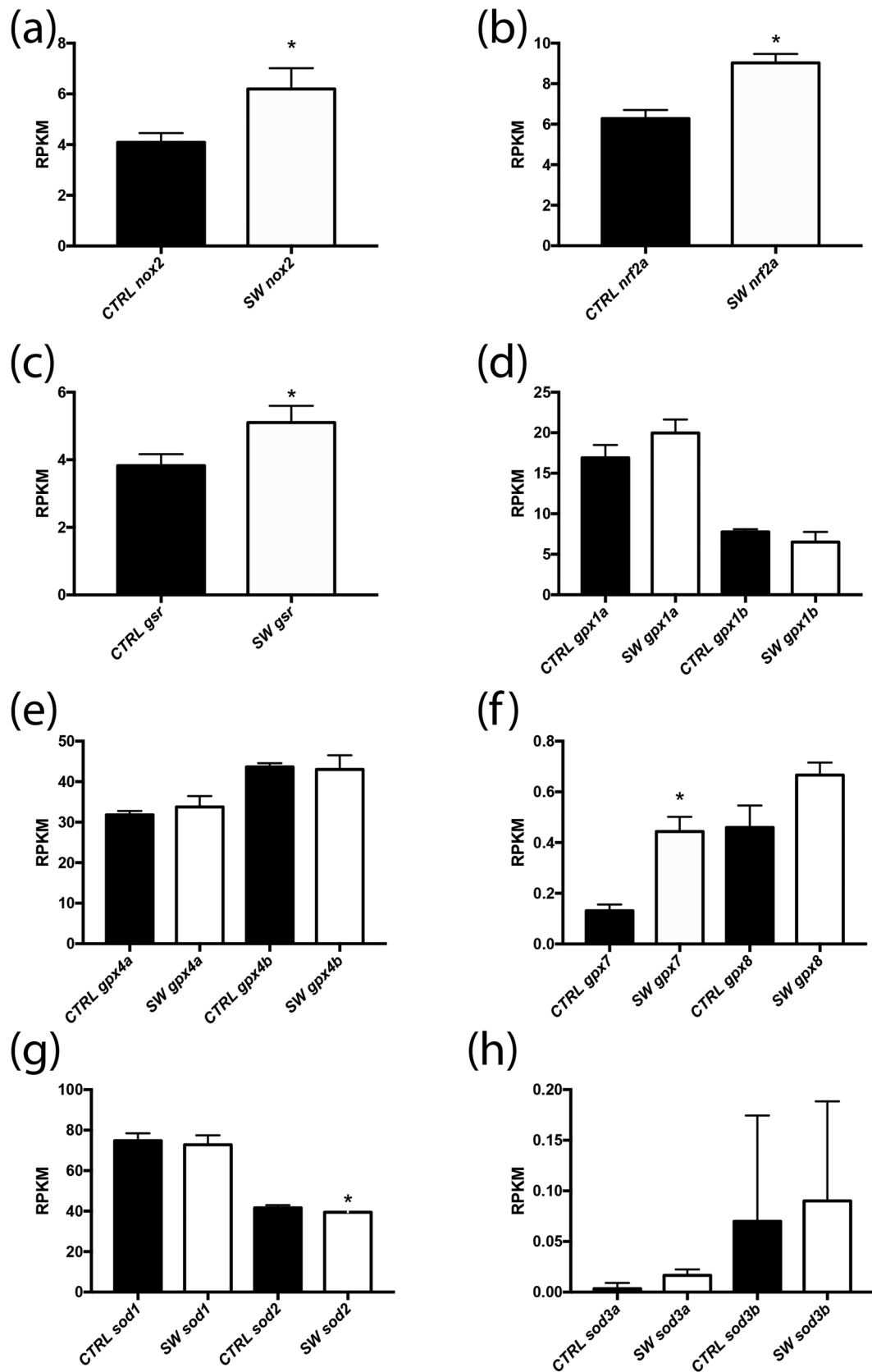


FIGURE 8 Expression of genes involved in oxidative stress and antioxidant defense during brain injury. (a–h) *nox2*, *nrf2a*, *gsr* (glutathione reductase), *gpx*, and *sod* gene expression in the control (CTRL) and stab-wounded (SW) telencephalic hemisphere 5 days after brain injury. Reanalysis of the RNA sequencing data set from injured and uninjured zebrafish telencephalon at 5 dpl from Rodriguez Viales et al. (2015) and Gourain et al. (2021). Enriched microglia genes are upregulated at 5 days post-brain injury. * $p < .05$

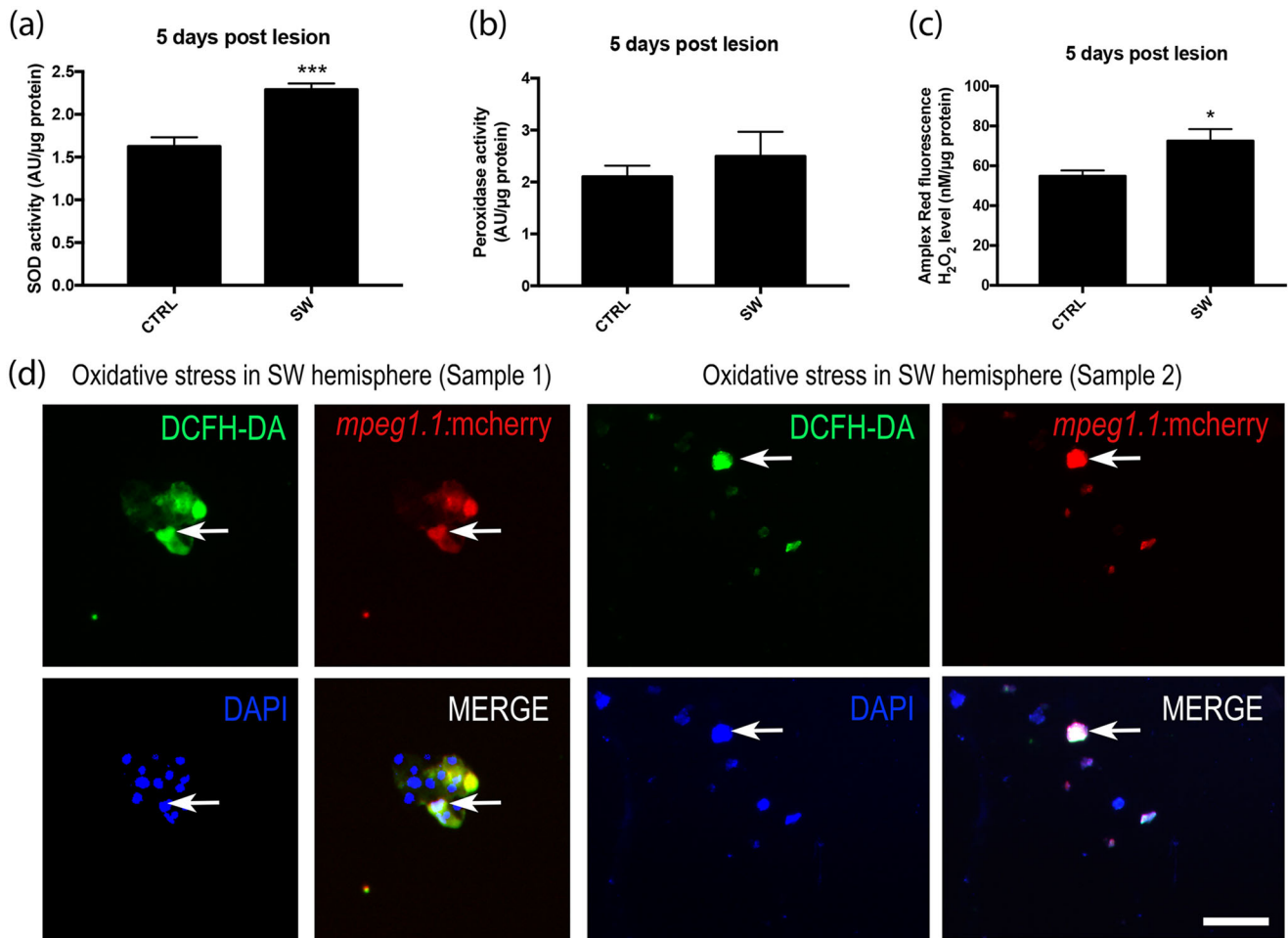


FIGURE 9 Antioxidant enzyme activities and oxidative stress after telencephalic injury. (a) Superoxide dismutase (SOD) activities from control (CTRL) and stab-wounded (SW) telencephalon at 5 dpl from two independent experiments showing a significant increased activity of the antioxidant SOD enzyme. (b) Peroxidase activity from control and stab-wounded telencephalon. An increasing trend was observed in two independent experiments in the injured telencephalon but remains not significant. (c) Amplex Red fluorescence showing a significant increase in H_2O_2 levels in the injured telencephalon compared to the respective control at 5 dpl. (d) Representative pictures of dissociated cells from 5 dpl telencephala showing DCFH-DA staining in mpeg1.1:mCherry-positive microglia/immune cells (arrows). $n = 3-6$ pools of 5 CTRL and SW telencephalon. * $p < .05$; *** $p < .001$. Bar: 25 μm

density and its correct migration in the brain. The *csf1r* (colony-stimulating factor 1 receptor) genes have been shown to play a key role in the density and distribution of microglia in the optic tectum (Oosterhof et al., 2018). However, *csf1r* involvement in other brain regions is largely unknown.

4.2 | Microglia display different phenotypes in the brain of adult zebrafish

In our study, different types of microglia have been reported in homeostatic conditions (i) elongated microglia mainly localized along blood vessels, (ii) rounded/amoeboid microglia mostly localized in the vicinity of cerebral ventricles known to correspond to neurogenic niches, and (iii) ramified and hyper-ramified microglia that were found for a high proportion in the diencephalon and midbrain. The roles of these different microglia subtypes are still not known in the healthy zebrafish brain.

Elongated microglia were mainly associated with endothelial cells (Figure 4). In mammals, microglia participate in the establishment and physiology of the BBB, allowing, among other things, its opening to promote leukocyte extravasation and angiogenesis (Dudvarski Stankovic et al., 2016). Consequently, it would be interesting to further investigate the role of zebrafish microglia in the maintenance and/or function of the blood-brain barrier. These blood vessel-associated microglia could also correspond to migratory microglia using the vasculature to reach their destination, as it has been shown in mice (Mondo et al., 2020), and/or participate in neurovascular unit complexes (Schaeffer & Iadecola, 2021).

The presence of rounded/amoeboid microglia associated with NSCs in the ventricular zone has also been observed. Similar data have also been reported in some ventricular regions in mice, as well as in the subventricular zone of the lateral ventricle, corresponding to a major neurogenic niche in adult mammals (Ribeiro Xavier et al., 2015; Tan et al., 2020). These data suggest a possible role of microglia in the regulation of neurogenic processes in healthy conditions. In mammals,

microglia have been described for modulating NSC proliferation, new neuron differentiation, and synaptogenesis (Sato, 2015; Diaz-Aparicio et al., 2020; Araki et al., 2021; Perez-Rodriguez et al., 2021). They participate in the clearance and removal of cells, the regulation of neural progenitor differentiation into neuroblasts, their survival, and functional integration (Ribeiro Xavier et al., 2015; Rodriguez-Iglesias et al., 2019; Al-Onaizi et al., 2020; Diaz-Aparicio et al., 2020). So far, in addition to their scavenger roles, microglia are implied in brain remodeling and plasticity of neural circuits (Paolicelli et al., 2011; Paladini et al., 2021). Such features would benefit further investigation in fish.

Regarding ramified microglia, they appear more numerous in the posterior part of the brain where they coexist with amoeboid microglia. In the midbrain, Wu et al. (2020) showed that ccl34b.1-negative microglia have branched processes, low mobility, and phagocytic characteristics. They also demonstrated that ccl34b.1-positive microglia were the predominant population in the midbrain and exhibited amoeboid, motile, and phagocytic properties (Wu et al., 2020). Also, in zebrafish larvae and young fish (7- and 28-day postfertilization), it was shown that in the posterior brain, ramified microglia were increased in synaptic regions of the midbrain and hindbrain, while amoeboid microglia were detected in the optic tectum around neurogenic zones (Silva et al., 2021). We also observed amoeboid microglia along the different neurogenic areas of the whole brain. These data suggest that different types of microglia could mediate synaptic remodeling and cell engulfment.

This diversity in microglia density and phenotype in the adult zebrafish brain is to be compared with the situation in mammals. Indeed, in mice, the number of microglia, their morphology, their molecular signature, and their functions differ among brain areas (Tan et al., 2020). This suggests that different phenotypes might also contribute to different microglial functions in fish, as shown by Wu et al. (2020) in the zebrafish midbrain.

4.3 | Microglia/immune cell recruitment and oxidative stress after telencephalic injury

After any type of brain injury, inflammatory and oxidative stresses occur, leading to a disruption of brain homeostasis (Rodríguez-Rodríguez et al., 2014). Under such conditions, microglia mediate oxidative and inflammatory processes. In zebrafish, after stab wounding of the telencephalon, microglia are rapidly activated and recruited to the wound site (März et al., 2011; Baumgart et al., 2012; Kyritsis et al., 2012; Diotel et al., 2020; Ghaddar, Lubke, et al., 2021). Moreover, peripheral immune cells can enter within the brain parenchyma due to BBB breakdown. The number of microglia/immune cells recruited to the injured telencephalon increases from 4 to 6 h after injury, peaking at around 1–3 days depending on the microglia marker used for tracing these cells and then slowly decreases. It nevertheless remains significantly elevated at 3–4 dpl in the injured telencephalon compared to the control telencephalon (März et al., 2011; Baumgart et al., 2012; Kyritsis et al., 2012; Kanagaraj et al., 2020; Ghaddar, Lubke, et al., 2021). At 5 dpl, a key time point for regenerative neurogenesis (März

et al., 2011; Baumgart et al., 2012; Kyritsis et al., 2012; Kanagaraj et al., 2020; Ghaddar, Lubke, et al., 2021), we demonstrated that the number of mpeg1.1:mCherry-positive cells remained significantly higher in the injured hemisphere than in the control one (Figure 6). These data were supported by L-plastin immunohistochemistry (data not shown) and by reanalysis of RNAseq data sets, demonstrating the upregulation of genes enriched in microglia (Figure 6).

The inflammatory processes taking place during zebrafish brain damage induce regenerative neurogenesis (Kyritsis et al., 2012), and recent data suggest that this injury-induced neurogenesis was microglia dependent (Kanagaraj et al., 2020). Nevertheless, brain inflammation appears to be transient with a fast upregulation of pro-inflammatory cytokines that is coming back to basal levels in as early as 1 dpl (Kyritsis et al., 2012).

Until recently, only few data were available concerning oxidative stress process during brain regeneration in fish. The injection of the fluorescent oxidative stress probe DCFH-DA prior to stab wound injury resulted in a strong fluorescence staining 30 min after the lesion (Figure 7). However, at 5 dpl, no fluorescence staining was observed (data not shown). We hypothesized that the lack of fluorescence might be due to the inability of the probe to reach the brain tissue once brain repair had begun. Alternatively, the dissociation of cells from 5 dpl telencephalon and their incubation with DCFH-DA probes revealed that mpeg1.1:mCherry positive cells (microglia/immune cells) are a source of oxidative stress. In addition, we analyzed oxidative stress-related genes and performed the Amplex Red assay on the stabbed hemispheres. The *nox2* and *nrf2a* genes were upregulated, showing the persistence of a pro-oxidative environment at 5 days. This was confirmed by the increase in H₂O₂ levels revealed by the Amplex Red assay and by the increased SOD activity, an antioxidant enzyme known to be upregulated under pro-oxidative conditions. These last results are in agreement with the recent study by Anand et al. (2021) showing that stab wounding of the zebrafish telencephalon leads to a significant increase in SOD activity at 1 and 4 dpl, correlated with a significant increase in lipid peroxidation and reduced levels of glutathione (GSH). Interestingly, we showed the significant upregulation of the *glutathione reductase* gene. Indeed, glutathione reductase catalyzes the reduction of glutathione disulfide (GSSG, the oxidized form of glutathione) to glutathione in the sulfhydryl form (GSH, the reduced form), participating in the resistance to oxidative stress and the maintenance of a reducing environment. Thus, the work of Anand et al. (2021) and ours suggest that the expression of the glutathione reductase enzyme is increased during brain repair and leads to higher amount of GSH (glutathione) that is an antioxidant species preventing cell damage caused by ROS (Pompella et al., 2003). In parallel, Anand et al. also demonstrated that catalase activity increased only transiently at 1 dpl before reaching normal levels at 4 dpl. In our series of experiments, we were unfortunately unable to monitor catalase activity. Interestingly, although the GPx activity remains nonsignificant, it tended to be increased in two independent experiments. Possibly, the size of our sampling could be increased to limit individual response and the differences of the damaged areas.

Overall, these data suggest the persistence of a pro-oxidative environment at 5 dpl and point to microglia/immune cells as a main source of oxidative stress during brain repair. It raises questions about the role of oxidative stress and microglia/immune cells in brain repair mechanisms, involving among others cell survival and activation of regenerative neurogenesis, as well as the occurrence of oxidative stress in the cytoplasm or in mitochondria. Further functional studies would be needed to determine the actual beneficial or detrimental effects of oxidative stress during zebrafish brain regeneration through the inhibition of oxidative stress during brain repair mechanisms. Thus, it would be interesting to inhibit oxidative stress following brain injury to analyze microgliosis, cell survival, NSC proliferation, and newborn neuron migration.

5 | CONCLUSION

In this work, we provided a general mapping of microglia and reported different densities and morphologies of microglia in the healthy brain of adult zebrafish. We highlighted the proximity of microglia with endothelial cells and NSCs. These neuroanatomical observations raise the question of the possible role of microglia in BBB and neurogenic functions in the brain of adult zebrafish. Finally, we showed that at 5 dpl, microglia/immune cells are still abundantly present at the injury site with persistent oxidative stress in the injured hemisphere as shown by the analysis of different markers such as *nox2* and *nrf2a* and antioxidant defense activities. This work paves the way for further research on the links between microglia and oxidative stress on brain repair, notably in neurogenesis. Moreover, it opens the way to further research and the possible interaction between microglia, endothelial, and NSCs and their possible roles on BBB and neurogenic functions.

AUTHOR CONTRIBUTIONS

Conceptualization: Nicolas Diotel, Philippe Rondeau, Christian Lefebvre d'Hellencourt, Emmanuel Bourdon, Laura Gence, Danielle Fernezelian, and Sepand Rastegar; data curation: Nicolas Diotel and Sepand Rastegar; formal analysis: Nicolas Diotel, Philippe Rondeau, Christian Lefebvre d'Hellencourt, Emmanuel Bourdon, Sai Sandhya Narra, Sepand Rastegar, Laura Gence, and Danielle Fernezelian; funding acquisition: Nicolas Diotel; investigation: all authors. Writing original draft: Nicolas Diotel, Philippe Rondeau, Laura Gence, and Danielle Fernezelian; writing-review and editing: all authors. All the authors have read and agreed to the published version of the manuscript.

ACKNOWLEDGMENTS

We thank Matthieu Bringart for excellent technical support with the fish facility, as well as Dr. M. Redd for kindly providing the L-plastin antibody. This work was supported by grants from the University of La Réunion, European Union (EU)-Région Réunion-French State national counterpart: FEDER RE0022527 (ZEBRATOX).

CONFLICTS OF INTEREST

The authors declare no conflicts of interest.

DATA AVAILABILITY STATEMENT

The data that support the findings of this study are available on request from the corresponding author. The data are not publicly available due to privacy or ethical restrictions.

ORCID

Sepand Rastegar  <https://orcid.org/0000-0003-4411-5646>

Nicolas Diotel  <https://orcid.org/0000-0003-2032-518X>

REFERENCES

- Al-Onaizi, M., Al-Khalifah, A., Qasem, D., & ElAli, A. (2020). Role of microglia in modulating adult neurogenesis in health and neurodegeneration. *International Journal of Molecular Sciences*, 21(18), 6875.
- Alam, A., Thelin, E. P., Tajsic, T., Khan, D. Z., Khellaf, A., Patani, R., & Helmy, A. (2020). Cellular infiltration in traumatic brain injury. *Journal of Neuroinflammation*, 17(1), 328.
- Alunni, A., & Bally-Cuif, L. (2016). A comparative view of regenerative neurogenesis in vertebrates. *Development*, 143(5), 741–753.
- Anand, S. K., & Mondal, A. C. (2018). TrkB receptor antagonism inhibits stab injury induced proliferative response in adult zebrafish (*Danio rerio*) brain. *Neuroscience Letters*, 672, 28–33.
- Anand, S. K., & Mondal, A. C. (2020). Neuroanatomical distribution and functions of brain-derived neurotrophic factor in zebrafish (*Danio rerio*) brain. *Journal of Neuroscience Research*, 98(5), 754–763.
- Anand, S. K., Sahu, M. R., & Mondal, A. C. (2021). Induction of oxidative stress and apoptosis in the injured brain: Potential relevance to brain regeneration in zebrafish. *Molecular Biology Reports*, 48(6), 5099–5108.
- Araki, T., Ikegaya, Y., & Koyama, R. (2021). The effects of microglia- and astrocyte-derived factors on neurogenesis in health and disease. *The European Journal of Neuroscience*, 54(5), 5880–5901.
- Baumgart, E. V., Barbosa, J. S., Bally-Cuif, L., Gotz, M., & Ninkovic, J. (2012). Stab wound injury of the zebrafish telencephalon: A model for comparative analysis of reactive gliosis. *Glia*, 60(3), 343–357.
- Bhattarai, P., Cosacak, M. I., Mashkaryan, V., Demir, S., Popova, S. D., Govindarajan, N., Brandt, K., Zhang, Y., Chang, W., Ampatzis, K., & Kizil, C. (2020). Neuron-glia interaction through Serotonin-BDNF-NGFR axis enables regenerative neurogenesis in Alzheimer's model of adult zebrafish brain. *PLoS Biology*, 18(1), e3000585.
- Bhattarai, P., Thomas, A. K., Cosacak, M. I., Papadimitriou, C., Mashkaryan, V., Froc, C., Reinhardt, S., Kurth, T., Dahl, A., Zhang, Y., & Kizil, C. (2016). IL4/STAT6 signaling activates neural stem cell proliferation and neurogenesis upon Amyloid-beta42 aggregation in adult zebrafish brain. *Cell Reports*, 17(4), 941–948.
- Bhattarai, P., Thomas, A. K., Zhang, Y., & Kizil, C. (2017). The effects of aging on Amyloid-beta42-induced neurodegeneration and regeneration in adult zebrafish brain. *Neurogenesis (Austin)*, 4(1), e1322666.
- Cacialli, P. (2021). Neurotrophins time point intervention after traumatic brain injury: From zebrafish to human. *International Journal of Molecular Sciences*, 22(4), 1585.
- Cacialli, P., D'Angelo, L., Kah, O., Coumilleau, P., Gueguen, M. M., Pellegrini, E., & Lucini, C. (2018). Neuronal expression of brain derived neurotrophic factor in the injured telencephalon of adult zebrafish. *The Journal of Comparative Neurology*, 526(4), 569–582.
- Casano, A. M., Albert, M., & Peri, F. (2016). Developmental apoptosis mediates entry and positioning of microglia in the zebrafish brain. *Cell Reports*, 16(4), 897–906.

- Cassam-Sulliman, N., Ghaddar, B., Gence, L., Patche, J., Rastegar, S., Meilhac, O., & Diotel, N. (2021). HDL biodistribution and brain receptors in zebrafish, using HDLs as vectors for targeting endothelial cells and neural progenitors. *Scientific Reports*, 11(1), 6439.
- Diaz-Aparicio, I., Paris, I., Sierra-Torre, V., Plaza-Zabala, A., Rodriguez-Iglesias, N., Marquez-Ropero, M., Beccari, S., Hugueta, P., Abiega, O., Alberdi, E., Matute, C., Bernales, I., Schulz, A., Otrokocsi, L., Sperlagh, B., Happonen, K. E., Lemke, G., Maletic-Savatic, M., Valero, J., & Sierra, A. (2020). Microglia actively remodel adult hippocampal neurogenesis through the phagocytosis secretome. *The Journal of Neuroscience: The Official Journal of The Society for Neuroscience*, 40(7), 1453–1482.
- Diotel, N., Lubke, L., Strahle, U., & Rastegar, S. (2020). Common and distinct features of adult neurogenesis and regeneration in the telencephalon of zebrafish and mammals. *Frontiers in Neuroscience*, 14, 568930.
- Diotel, N., Vaillant, C., Gabbero, C., Mironov, S., Fostier, A., Gueguen, M. M., Anglade, I., Kah, O., & Pellegrini, E. (2013). Effects of estradiol in adult neurogenesis and brain repair in zebrafish. *Hormones and Behavior*, 63(2), 193–207.
- Dobi, A., Bravo, S. B., Veeren, B., Paradelo-Dobarro, B., Alvarez, E., Meilhac, O., Viranaicken, W., Baret, P., Devin, A., & Rondeau, P. (2019). Advanced glycation end-products disrupt human endothelial cells redox homeostasis: New insights into reactive oxygen species production. *Free Radical Research*, 53(2), 150–169.
- Dorsemans, A. C., Lefebvre d'Hellencourt, C., Ait-Arsa, I., Jestin, E., Meilhac, O., & Diotel, N. (2017). Acute and chronic models of hyperglycemia in zebrafish: A method to assess the impact of hyperglycemia on neurogenesis and the biodistribution of radiolabeled molecules. *Journal of Visualized Experiments*, (124), 55203. <https://doi.org/10.3791/55203>
- Dorsemans, A. C., Soule, S., Weger, M., Bourdon, E., Lefebvre d'Hellencourt, C., Meilhac, O., & Diotel, N. (2017). Impaired constitutive and regenerative neurogenesis in adult hyperglycemic zebrafish. *The Journal of Comparative Neurology*, 525(3), 442–458.
- Dudvarski Stankovic, N., Teodorczyk, M., Ploen, R., Zipp, F., & Schmidt, M. H. H. (2016). Microglia-blood vessel interactions: A double-edged sword in brain pathologies. *Acta Neuropathologica*, 131(3), 347–363.
- Eastman, C. L., D'Ambrosio, R., & Ganesh, T. (2020). Modulating neuroinflammation and oxidative stress to prevent epilepsy and improve outcomes after traumatic brain injury. *Neuropharmacology*, 172, 107907.
- Everse, J., Johnson, M. C., & Marini, M. A. (1994). Peroxidative activities of hemoglobin and hemoglobin derivatives. *Methods in Enzymology*, 231, 547–561.
- Fischer, R., & Maier, O. (2015). Interrelation of oxidative stress and inflammation in neurodegenerative disease: Role of TNF. *Oxidative Medicine and Cellular Longevity*, 2015, 610813.
- Ghaddar, B., Bringart, M., Lefebvre d'Hellencourt, C., Meilhac, O., & Diotel, N. (2021). Deleterious effects of overfeeding on brain homeostasis and plasticity in adult zebrafish. *Zebrafish*, 18(3), 190–206.
- Ghaddar, B., Lubke, L., Couret, D., Rastegar, S., & Diotel, N. (2021). Cellular mechanisms participating in brain repair of adult zebrafish and mammals after injury. *Cells*, 10(2), 391.
- Ginhoux, F., Lim, S., Hoeffel, G., Low, D., & Huber, T. (2013). Origin and differentiation of microglia. *Frontiers in Cellular Neuroscience*, 7, 45.
- Gourain, V., Armant, O., Lubke, L., Diotel, N., Rastegar, S., & Strahle, U. (2021). Multi-dimensional transcriptome analysis reveals modulation of cholesterol metabolism as highly integrated response to brain injury. *Frontiers in Neuroscience*, 15, 671249.
- Hameed, L. S., Berg, D. A., Belnoue, L., Jensen, L. D., Cao, Y., & Simon, A. (2015). Environmental changes in oxygen tension reveal ROS-dependent neurogenesis and regeneration in the adult newt brain. *eLife*, 4, e08422.
- Kanagaraj, P., Chen, J. Y., Skaggs, K., Qadeer, Y., Conner, M., Cutler, N., Richmond, J., Kommidu, V., Poles, A., Affrunti, D., Powell, C., Goldman, D., & Parent, J. (2020). Microglia stimulate zebrafish brain repair via a specific inflammatory cascade. *BioRxiv*, 79(3), 268–280.
- Kim, Y. S., & Joh, T. H. (2006). Microglia, major player in the brain inflammation: Their roles in the pathogenesis of Parkinson's disease. *Experimental & Molecular Medicine*, 38(4), 333–347.
- Kishimoto, N., Shimizu, K., & Sawamoto, K. (2012). Neuronal regeneration in a zebrafish model of adult brain injury. *Disease Models & Mechanisms*, 5(2), 200–209.
- Kroehne, V., Freudenreich, D., Hans, S., Kaslin, J., & Brand, M. (2011). Regeneration of the adult zebrafish brain from neurogenic radial glia-type progenitors. *Development*, 138(22), 4831–4841.
- Kyritsis, N., Kizil, C., Zocher, S., Kroehne, V., Kaslin, J., Freudenreich, D., Iltzsche, A., & Brand, M. (2012). Acute inflammation initiates the regenerative response in the adult zebrafish brain. *Science*, 338(6112), 1353–1356.
- Lawson, N. D., & Weinstein, B. M. (2002). In vivo imaging of embryonic vascular development using transgenic zebrafish. *Developmental Biology*, 248(2), 307–318.
- Lin, M. C., Liu, C. C., Liao, C. S., & Ro, J. H. (2021). Neuroprotective effect of quercetin during cerebral ischemic injury involves regulation of essential elements, transition metals, cu/zn ratio, and antioxidant activity. *Molecules*, 26(20), 6128.
- März, M., Chapouton, P., Diotel, N., Vaillant, C., Hesel, B., Takamiya, M., Lam, C. S., Kah, O., Bally-Cuif, L., & Strahle, U. (2010). Heterogeneity in progenitor cell subtypes in the ventricular zone of the zebrafish adult telencephalon. *Glia*, 58(7), 870–888.
- März, M., Schmidt, R., Rastegar, S., & Strahle, U. (2011). Regenerative response following stab injury in the adult zebrafish telencephalon. *Developmental Dynamics: An Official Publication of the American Association of Anatomists*, 240(9), 2221–2231.
- Miller, C. J., Gounder, S. S., Kannan, S., Goutam, K., Muthusamy, V. R., Firpo, M. A., Symons, J. D., Paine, R., 3rd, Hoidal, J. R., & Rajasekaran, N. S. (2012). Disruption of Nrf2/ARE signaling impairs antioxidant mechanisms and promotes cell degradation pathways in aged skeletal muscle. *Biochimica et Biophysica Acta*, 1822(6), 1038–1050.
- Miyamoto, N., Maki, T., Pham, L. D., Hayakawa, K., Seo, J. H., Mandeville, E. T., Mandeville, J. B., Kim, K. W., Lo, E. H., & Arai, K. (2013). Oxidative stress interferes with white matter renewal after prolonged cerebral hypoperfusion in mice. *Stroke*, 44(12), 3516–3521.
- Mondo, E., Becker, S. C., Kautzman, A. G., Schifferer, M., Baer, C. E., Chen, J., Huang, E. J., Simons, M., & Schafer, D. P. (2020). A developmental analysis of juxtavascular microglia dynamics and interactions with the vasculature. *The Journal of Neuroscience: The Official Journal of The Society for Neuroscience*, 40(34), 6503–6521.
- Mugoni, V., Camporeale, A., & Santoro, M. M. (2014). Analysis of oxidative stress in zebrafish embryos. *Journal of Visualized Experiments*, (89), 51328. <https://doi.org/10.3791/51328>
- Nayak, D., Roth, T. L., & McGavern, D. B. (2014). Microglia development and function. *Annual Review of Immunology*, 32, 367–402.
- Oosterhof, N., Holtman, I. R., Kuil, L. E., van der Linde, H. C., Boddeke, E. W., Eggen, B. J., & van Ham, T. J. (2017). Identification of a conserved and acute neurodegeneration-specific microglial transcriptome in the zebrafish. *Glia*, 65(1), 138–149.
- Oosterhof, N., Kuil, L. E., van der Linde, H. C., Burm, S. M., Berdowski, W., van Ijcken, W. F. J., van Swieten, J. C., Hol, E. M., Verheijen, M. H. G., & van Ham, T. J. (2018). Colony-Stimulating factor 1 receptor (CSF1R) regulates microglia density and distribution, but not microglia differentiation in vivo. *Cell Reports*, 24(5), 1203–1217.e1206.
- Paladini, M. S., Feng, X., Krukowski, K., & Rosi, S. (2021). Microglia depletion and cognitive functions after brain injury: From trauma to galactic cosmic ray. *Neuroscience Letters*, 741, 135462.
- Paolicelli, R. C., Bolasco, G., Pagani, F., Maggi, L., Scianni, M., Panzanelli, P., Giustetto, M., Ferreira, T. A., Guiducci, E., Dumas, L., Ragozzino, D., & Gross, C. T. (2011). Synaptic pruning by microglia is necessary for normal brain development. *Science*, 333(6048), 1456–1458.
- Pellegrini, E., Mouriec, K., Anglade, I., Menuet, A., Le Page, Y., Gueguen, M. M., Marmignon, M. H., Brion, F., Pakdel, F., & Kah, O. (2007).

- Identification of aromatase-positive radial glial cells as progenitor cells in the ventricular layer of the forebrain in zebrafish. *The Journal of Comparative Neurology*, 501(1), 150–167.
- Perez-Rodriguez, D. R., Blanco-Luquin, I., & Mendioroz, M. (2021). The participation of microglia in neurogenesis: A review. *Brain Sciences*, 11(5). <https://doi.org/10.3390/brainsci11050658>
- Pompella, A., Visvikis, A., Paolicchi, A., De Tata, V., & Casini, A. F. (2003). The changing faces of glutathione, a cellular protagonist. *Biochemical Pharmacology*, 66(8), 1499–1503.
- Praveen Kumar, P., Madhuri D., Siva Sankar Reddy, L., Dastagiri Reddy, Y., Somasekhar, G., Sirisha, N. V. L., Nagaraju, K., Shouib, M. S., & Rizwaan, A. S. (2021). A new cerebral ischemic injury model in rats, preventive effect of gallic acid and in silico approaches. *Saudi Journal of Biological Sciences*, 28(9), 5204–5213.
- Redd, M. J., Kelly, G., Dunn, G., Way, M., & Martin, P. (2006). Imaging macrophage chemotaxis in vivo: Studies of microtubule function in zebrafish wound inflammation. *Cell Motility and the Cytoskeleton*, 63(7), 415–422.
- Rhee, S. G., Chang, T. S., Jeong, W., & Kang, D. (2010). Methods for detection and measurement of hydrogen peroxide inside and outside of cells. *Molecules and Cells*, 29(6), 539–549.
- Ribeiro Xavier, A. L., Kress, B. T., Goldman, S. A., Lacerda de Menezes, J. R., & Nedergaard, M. (2015). A distinct population of microglia supports adult neurogenesis in the subventricular zone. *The Journal of Neuroscience: The Official Journal of The Society for Neuroscience*, 35(34), 11848–11861.
- Rodriguez Viales, R., Diotel, N., Ferg, M., Armant, O., Eich, J., Alunni, A., Marz, M., Bally-Cuif, L., Rastegar, S., & Strahle, U. (2015). The helix-loop-helix protein id1 controls stem cell proliferation during regenerative neurogenesis in the adult zebrafish telencephalon. *Stem Cells*, 33(3), 892–903.
- Rodriguez-Iglesias, N., Sierra, A., & Valero, J. (2019). Rewiring of memory circuits: Connecting adult newborn neurons with the help of microglia. *Frontiers in Cell and Developmental Biology*, 7, 24.
- Rodriguez-Rodriguez, A., Egea-Guerrero, J. J., Murillo-Cabezas, F., & Carrillo-Vico, A. (2014). Oxidative stress in traumatic brain injury. *Current Medicinal Chemistry*, 21(10), 1201–1211.
- Sakai, S., & Shichita, T. (2019). Inflammation and neural repair after ischemic brain injury. *Neurochemistry International*, 130, 104316.
- Sato, K. (2015). Effects of microglia on neurogenesis. *Glia*, 63(8), 1394–1405.
- Schaeffer, S., & Iadecola, C. (2021). Revisiting the neurovascular unit. *Nature Neuroscience*, 24(9), 1198–1209.
- Schmidt, R., Beil, T., Strähle, U., & Rastegar, S. (2014). Stab wound injury of the zebrafish adult telencephalon: A method to investigate vertebrate brain neurogenesis and regeneration. *Journal of Visualized Experiments*, (90), e51753. <https://doi.org/10.3791/51753>
- Sierra, A., de Castro, F., Del Rio-Hortega, J., Rafael Iglesias-Rozas, J., Garrosa, M., & Kettenmann, H. (2016). The “Big-Bang” for modern glial biology: Translation and comments on pio del rio-hortega 1919 series of papers on microglia. *Glia*, 64(11), 1801–1840.
- Silva, N. J., Dorman, L. C., Vainchtein, I. D., Horneck, N. C., & Molofsky, A. V. (2021). In situ and transcriptomic identification of microglia in synapse-rich regions of the developing zebrafish brain. *Nature Communications*, 12(1), 5916.
- Silva, N. J., Nagashima, M., Li, J., Kakuk-Atkins, L., Ashrafzadeh, M., Hyde, D. R., & Hitchcock, P. F. (2020). Inflammation and matrix metalloproteinase 9 (Mmp-9) regulate photoreceptor regeneration in adult zebrafish. *Glia*, 68(7), 1445–1465.
- Simpson, D. S. A., & Oliver, P. L. (2020). ROS generation in microglia: Understanding oxidative stress and inflammation in neurodegenerative disease. *Antioxidants (Basel)*, 9(8). <https://doi.org/10.3390/antiox9080743>
- Sipka, T., Peroceschi, R., Hassan-Abdi, R., Gross, M., Ellett, F., Begon-Pescia, C., Gonzalez, C., Lutfalla, G., & Nguyen-Chi, M. (2021). Damage-Induced calcium signaling and reactive oxygen species mediate macrophage activation in Zebrafish. *Frontiers in Immunology*, 12, 636585.
- Slemmer, J. E., Shacka, J. J., Sweeney, M. I., & Weber, J. T. (2008). Antioxidants and free radical scavengers for the treatment of stroke, traumatic brain injury and aging. *Current Medicinal Chemistry*, 15(4), 404–414.
- Smith, J. A., Das, A., Ray, S. K., & Banik, N. L. (2012). Role of pro-inflammatory cytokines released from microglia in neurodegenerative diseases. *Brain Research Bulletin*, 87(1), 10–20.
- Stence, N., Waite, M., & Dailey, M. E. (2001). Dynamics of microglial activation: A confocal time-lapse analysis in hippocampal slices. *Glia*, 33(3), 256–266.
- Tan, Y. L., Yuan, Y., & Tian, L. (2020). Microglial regional heterogeneity and its role in the brain. *Molecular Psychiatry*, 25(2), 351–367.
- Var, S. R., & Byrd-Jacobs, C. A. (2020). Role of macrophages and microglia in zebrafish regeneration. *International Journal of Molecular Sciences*, 21(13). <https://doi.org/10.3390/ijms21134768>
- Wu, S., Nguyen, L. T. M., Pan, H., Hassan, S., Dai, Y., Xu, J., & Wen, Z. (2020). Two phenotypically and functionally distinct microglial populations in adult zebrafish. *Science Advances*, 6(47). <https://doi.org/10.1126/sciadv.abd1160>
- Zambusi, A., & Ninkovic, J. (2020). Regeneration of the central nervous system—principles from brain regeneration in adult zebrafish. *World Journal of Stem Cells*, 12(1), 8–24.
- Zhang, Y., Chen, K., Sloan, S. A., Bennett, M. L., Scholze, A. R., O’Keeffe, S., Phatnani, H. P., Guarnieri, P., Caneda, C., Ruderisch, N., Deng, S., Liddelow, S. A., Zhang, C., Daneman, R., Maniatis, T., Barres, B. A., & Wu, J. Q. (2014). An RNA-sequencing transcriptome and splicing database of glia, neurons, and vascular cells of the cerebral cortex. *The Journal of Neuroscience: The Official Journal of The Society for Neuroscience*, 34(36), 11929–11947.
- Zhao, S., Zhang, L., Xu, Z., & Chen, W. (2013). Neurotoxic effects of iron overload under high glucose concentration. *Neural Regeneration Research*, 8(36), 3423–3433.
- Wullimann, M. F., Rupp, B., & Reichert, H. (1996). *Neuroanatomy of the zebrafish brain: A topological atlas* (pp. 1–144). Birkhäuser Verlag. <https://doi.org/10.1007/978-3-0348-8979-7>
- Menuet, A., Pellegrini, E., Brion, F., Gueguen, M. M., Anglade, I., Pakdel, F., & Kah, O. (2005). Expression and estrogen-dependent regulation of the zebrafish brain aromatase gene. *The Journal of Comparative Neurology*, 485(4), 304–20. Accession Number: 15803511 <https://doi.org/10.1002/cne.20497> <https://www.ncbi.nlm.nih.gov/pubmed/15803511>

SUPPORTING INFORMATION

Additional supporting information can be found online in the Supporting Information section at the end of this article.